Helsinki University of Technology

Optics and Molecular Materials

Espoo 2003

SPATIAL CORRELATIONS AND PARTIAL POLARIZATION IN ELECTROMAGNETIC OPTICAL FIELDS: EFFECTS OF EVANESCENT WAVES

Tero Setälä

TEKNILLINEN KORKEAKOULU
TEKNISKA HÖGSKOLAN
HELSINKI UNIVERSITY OF TECHNOLOGY
TECHNISCHE UNIVERSITÄT HELSINKI
UNIVERSITE DE TECHNOLOGIE D'HELSINKI

Helsinki University of Technology
Optics and Molecular Materials
Espoo 2003

SPATIAL CORRELATIONS AND PARTIAL POLARIZATION IN ELECTROMAGNETIC OPTICAL FIELDS: EFFECTS OF EVANESCENT WAVES

Tero Setälä

Dissertation for the degree of Doctor of Science in Technology to be presented with due permission of the Department of Engineering Physics and Mathematics for public examination and debate in Auditorium S4 at Helsinki University of Technology (Espoo, Finland) on the 28th of March, 2003, at 12 noon.

Helsinki University of Technology
Department of Engineering Physics and Mathematics
Optics and Molecular Materials

Teknillinen korkeakoulu
Teknillisen fysiikan ja matematiikan osasto
Optiikka ja molekyylimateriaalit

Distribution:
Helsinki University of Technology
Optics and Molecular Materials
P.O. Box 2200
FIN-02015 HUT
Tel. +358-9-451-3153
Fax. +358-9-451-3155
Available in pdf format at http://lib.hut.fi/Diss

ISBN 951-22-6402-1

Otamedia Oy
Espoo 2003

HELSINKI UNIVERSITY OF TECHNOLOGY P.O. BOX 1000, FIN-02015 HUT http://www.hut.fi	ABSTRACT OF DOCTORAL DISSERTATION

Author Tero Setälä

Name of the dissertation

SPATIAL CORRELATIONS AND PARTIAL POLARIZATION IN ELECTROMAGNETIC OPTICAL FIELDS: EFFECTS OF EVANESCENT WAVES

Date of manuscript 10.12.2002	Date of the dissertation 28.3.2003
☐ Monograph	☑ Article dissertation (summary + original articles)

Department	Department of Engineering Physics and Mathematics
Laboratory	Optics and Molecular Materials
Field of research	Near-field optics
Opponent(s)	Dr. Daniel F. V. James
Supervisor	Professor Matti Kaivola
(Instructor)	Professor Ari T. Friberg, Professor Matti Kaivola

Abstract

In this thesis, partial polarization and spatial correlation properties of electromagnetic optical fields are investigated. The emphasis is on near fields which exist only within the distance of the light wavelength from the emitting or scattering object. In the near-field region, the contribution of the evanescent (non-radiating) waves is overwhelming compared to the propagating waves that can be observed far from the source.

Certain fundamental issues related to the optical near-fields are studied. The decomposition of the free-space Green tensor into its evanescent and propagating parts is performed. This issue is of importance in near-field optics and it has attracted considerable attention in the recent literature. Another fundamental issue investigated in the thesis concerns the three-dimensional degree of polarization needed to characterize of electromagnetic fields having arbitrary planar or non-planar wave structures. The physical interpretation of the concept is presented, and its differences in comparison with the conventional two-dimensional formulation of the degree of polarization are brought out. The theory is applied to investigate the effects of evanescent waves and resonant surface waves on the polarization state of the near fields generated by some thermal half-space sources.

The thesis also includes a study of the partial polarization and spatial correlation properties of homogeneous free electromagnetic fields. The fields are modelled as an isotropic distribution of angularly uncorrelated and, in the 2D-sense, unpolarized plane waves propagating within a solid angle. When the solid angle extends over the full space, the spatial correlations are found to be determined by the imaginary part of the associated Green tensor, and the field is fully unpolarized in the 3D-sense. These results are the same as for black-body fields, although here no thermal equilibrium is assumed. The same behavior is discovered for any electromagnetic field generated by a statistically homogeneous and isotropic current distribution, which fluctuates within a medium having a vanishingly small absorption. For the fields whose electric cross-spectral density tensor is proportional to the imaginary part of the Green tensor, the degree of coherence has a universal form given by the sinc law.

Keywords optical near field, polarization, coherence	
UDC	Number of pages 44
ISBN (printed) 951-22-6401-3	ISBN (pdf) 951-22-6402-1
ISBN (others)	ISSN
Publisher Helsinki University of Technology	
Print distribution	
☑ The dissertation can be read at http://lib.hut.fi/Diss/	

Preface

The research summarized in this work has been carried out at the Materials Physics Laboratory and at the Optics and Molecular Materials Laboratory of Helsinki University of Technology in the Department of Engineering Physics and Mathematics in collaboration with the Optics Department of the Royal Institute of Technology, Stockholm.

I am indebted to my supervisors Prof. Matti Kaivola and Prof. Ari T. Friberg for their guidance and support during the course of this work. I thank them for teaching me a lot of scientific practise and providing inspiring ideas for manuscript preparation. I separately acknowledge Prof. Friberg for several fruitful visits that I had a chance to make to the Royal Institute. I am obliged to the people (present and former) in the *Miilu* laboratory for a humorous and lively working environment. I had a particularly pleasant time during the fishing tours that we made. I thank our laboratory secretary Ms. Orvokki Nyberg for arranging the practical matters.

I wish to express my gratitude to the Graduate School of Modern Optics and Photonics, the Academy of Finland, and the Helsinki University of Technology for funding my doctoral studies. Personal grants from the Jenny and Antti Wihuri Foundation, the Vilho, Yrjö and Kalle Väisälä Foundation, the Finnish Foundation of Technology and the Finnish Cultural Foundation are gratefully acknowledged. The Center of Scientific Computing (CSC) is also thanked for providing the computer resources.

I thank my friends for providing a nice counterbalance to my work. Special thanks go to Laura for her patience during this work.

Espoo, December 2002

Tero Setälä

List of Publications

This thesis is a review of the author's work on near-field optics and electromagnetic coherence theory. It consists of an overview and the following selection of the author's publications in these fields:

I. T. Setälä, M. Kaivola, and A. T. Friberg, "Decomposition of the point-dipole field into homogeneous and evanescent parts", *Phys. Rev. E* **59**, 1200–1206 (1999).

II. T. Setälä, A. Shevchenko, M. Kaivola, and A. T. Friberg, "Degree of polarization for optical near fields", *Phys. Rev. E* **66**, 016615 (2002).

III. T. Setälä, M. Kaivola, and A. T. Friberg, "Degree of polarization in near fields of thermal sources: effects of surface waves", *Phys. Rev. Lett.* **88**, 123902 (2002).

IV. T. Setälä, M. Kaivola, and A. T. Friberg, "Spatial correlations and degree of polarization in homogeneous electromagnetic fields", *Opt. Lett.*, submitted.

V. T. Setälä, K. Blomstedt, M. Kaivola, and A. T. Friberg, "Universality of electromagnetic-field correlations within homogeneous and isotropic sources", *Phys. Rev. E* **67**, 026613 (2003).

Throughout the overview, these papers will be referred to by Roman numerals.

Author's Contribution

The research presented in this dissertation is the result of the work on near-field optics and electromagnetic coherence theory carried out during the years 1997–2002 in the Materials Physics Laboratory (1997–2000), and in the new Optics and Molecular Materials Laboratory (2000–2002) of Helsinki University of Technology, in collaboration with the Optics Department of the Royal Institute of Technology in Stockholm.

The author has had a major role in all aspects of the research work. He has performed all the analytical and numerical calculations reported in Papers I-V, and has strongly contributed to the interpretation of the results. The author has written the first manuscripts of all the Papers. In addition to the contributed Papers, the author has reported the results in several international[1] and national[2] conferences.

[1] Electromagnetic Optics, Hyères, France, 1998; Electromagnetic Optics 2, Paris, France, 2001; The 7^{th} International Conference on Near-Field Optics and Related Techniques NFO-7, Rochester, NY, USA, 2002; 19^{th} Congress of the International Commission for Optics, Firenze, Italy, 2002.

[2] Annual Conference of the Finnish Physical Society, 1998–2002; Optics Days, 1998–2001.

Contents

1 Introduction

Nanophotonics deals with the controlled manipulation of optical near fields and their exploitation in investigations of nanometer-scale structures [1]. The near field is characterized by the evanescent optical waves, which are strong only within the distance of the wavelength of light from the surface of an emitting or scattering object. The evanescent waves play an essential role in the design and characterization of components for nanotechnology. For instance, in atom optics [2], they are used to build atom mirrors and guides, and in scanning near-field optical microscopy (SNOM) [3–7] they are utilized to study the optical properties of a sample with a spatial resolution surpassing the classical diffraction limit.

The SNOM technique has grown and developed into a mature tool to acquire subwavelength-scale optical information about nanostructures. The basic idea of SNOM is to use a nanoprobe to detect the evanescent field in the immediate vicinity of the sample. The most common probe type is a metal-coated, tapered optical fiber tip with a nanoaperture at the apex. The aperture acts as a local scattering center transforming some of the evanescent field components into propagating waves that can be detected in the far zone. By scanning the nanoprobe over the sample surface, the evanescent field distribution can be detected with a resolution limited mainly by the size of the nanoprobe and the scanning distance. In practice, the resolution achieved in a near-field measurement is on the order of a few tens of nanometers providing an improvement by an order of magnitude to the best conventional far-zone measurements. Optical near-field microscopy has become one of the standard techniques among the scanning-probe microscopies. It has found applications in a diversity of subfields of modern technology including, for example, characterization of optoelectronical components, and high-density data storage [4, 5], mapping of the optical properties of surfaces and thin films [8], nano- and single-molecule spectroscopy, and investigations of various biological samples [9, 10].

Several theoretical methods have been developed to model the optical near-field distribution in nano-scale structures [11]. For example, in the early near-field studies, perturbative diffraction theory based on plane-wave expansions was used to model the near fields above surfaces having periodic small-amplitude corrugations [12]. Multiple multipole (MMP) expansions, which in comparison with the plane-wave methods are better suited to deal with localized geometries, have been employed to calculate, for example, the field distribution inside a tapered metal-coated optical fiber tip of a near-field microscope [11]. The finite-difference time-domain (FDTD) method has been implemented for both two- and three dimensional SNOM modelling [13]. Furthermore, the boundary-element method for both TE and TM polarized light has been realized for investigations of the near-field distribution in

a two-dimensional tip-sample geometry of SNOM [14]. In particular, the Green tensor techniques, which are well suited to self-consistently treat the optical interaction in nano structures, such as the tip-sample interaction in SNOM, have become a widely used method in near-field studies [11]. Present theoretical methods are able to assess, for example, the influence of the polarization direction of light, scanning height of the nano probe, and of the geometries and the dielectric contrast of the materials to the measured near-field signal.

In theoretical near-field investigations the electromagnetic field is, as a rule, taken to be deterministic, i.e., fully coherent and polarized. However, the recent studies of the properties of partially coherent optical near fields have shown that the spectrum of the near field may differ from the spectrum of the source and of the far field. Also, the spatial correlation length in the near field may be much shorter than the wavelength or it may extend over several tens of wavelengths even for a thermal source, when resonant surface waves such as surface plasmon or phonon polaritons are excited. These extraordinary phenomena were discovered only a couple of years ago and they illustrate the potential of finding novel effects when the statistical nature of the electromagnetic field is taken into account in the near-field investigations. Coherence theory has so far mainly been applied to scattered or radiated far fields. For these studies the results and methods are well established, but in many cases they are not directly applicable to optical near fields, where the effects of evanescent waves become appreciable or even dominant. As a matter of fact, until lately, even such a fundamental quantity as the degree of polarization has not been defined for the near fields.

This compendium to the thesis is organized as follows: In Sec. 2, in order to facilitate the subsequent presentation, some basic concepts for analyzing fluctuating electromagnetic fields are provided. In Sec. 3, the electromagnetic field produced by a point-dipole source is decomposed into its evanescent and propagating parts [Paper I]. This subject is of fundamental importance for near-field optics, and it has attracted considerable attention in the recent literature. Although Sec. 3 comprises an exception to the general theme of the presentation in the sense that it deals with fully deterministic fields, it provides insight into the nature of the evanescent field, as well as introduces several concepts that are needed in the later sections.

Section 4, which constitutes the heart of the thesis, introduces a three-dimensional formalism to treat the degree of polarization [Paper II], which, unlike the conventional two-dimensional theory, is applicable to electromagnetic fields having arbitrary, planar or non-planar, wave structures. We also formulate the three-dimensional degree of polarization in terms of the generalized Stokes parameters and discuss the physical interpretation. Throughout the presentation the differences between the

two- and three dimensional formalisms are emphasized. The new three-dimensional formalism is applied to assess the partial polarization in near-fields produced by thermally fluctuating half-space sources, particularly in cases where the near field is strongly polarized owing to resonant surface plasmons or phonons [Paper III]. Besides near fields, the theory is also applied to study the partial polarization in statistically homogeneous free electromagnetic fields, which are modelled as superpositions of plane waves that are angularly uncorrelated, unpolarized (in the two-dimensional sense), and isotropically distributed within a cone of angles [Paper IV]. For these fields we also analyze their spatial correlation properties.

Section 5 discusses the spatial correlation properties of electromagnetic fields produced by statistically homogeneous and isotropic sources [Paper V]. For any such field in a low-loss medium the correlation properties are found to be determined by the associated Green tensor, i.e., by the propagation properties in the medium, and not by the source characteristics. The known behavior of black-body fields is recovered, but the results apply to a wider class of sources, which are not necessarily in thermal equilibrium. The behavior of correlations is explained within the same plane-wave model for which the spatial correlations and partial polarization are analyzed in Sec. 4.

2 Basic Concepts

The basic quantities in the theory of electromagnetic fields, the current and charge densities and the electric and magnetic fields, are never exactly deterministic, but include some random fluctuations. In order to analyze the fluctuating electromagnetic fields, it is necessary to employ tools provided by the optical coherence theory [15–19]. In this section, a brief overview of the basic concepts of the second-order electromagnetic coherence theory, both in the space-time and space-frequency domain, will be given. The emphasis is on the spectral treatment, and in particular on the topics that are employed in Papers II-V.

2.1 Complex analytic signal representation

Throughout our analysis, the random quantities are taken to be stationary with zero mean. Stationarity reflects the fact that the character of the fluctuations does not change with time, and the zero-mean is required to avoid possible singularities in the spectral quantities. We denote the realization of a fluctuating vector quantity, at a point $\mathbf{r}$ and at time t, by $\mathbf{F}^{(r)}(\mathbf{r},t)$. The vector $\mathbf{F}^{(r)}(\mathbf{r},t)$ is a real function of position and time, as indicated by the superscript, and it may stand for either the electric or magnetic field vector or for the current density. In the Fourier representation, $\mathbf{F}^{(r)}(\mathbf{r},t)$ takes the form

$$\mathbf{F}^{(r)}(\mathbf{r},t)=\int_{-\infty}^{\infty}\tilde{\mathbf{F}}(\mathbf{r},\omega)e^{-i\omega t}d\omega, \tag{1}$$

where ω denotes the frequency. Since $\mathbf{F}^{(r)}(\mathbf{r},t)$ is real, the negative and positive frequency components of the (generally complex) spectral amplitudes satisfy the relation $\tilde{\mathbf{F}}(\mathbf{r},-\omega)=\tilde{\mathbf{F}}^{*}(\mathbf{r},\omega)$. We see that no extra information is included in the negative frequency components that would not already exist in the positive ones. With this notion, one is led to introducing the complex vector

$$\mathbf{F}(\mathbf{r},t)=\int_{0}^{\infty}\tilde{\mathbf{F}}(\mathbf{r},\omega)e^{-i\omega t}d\omega, \tag{2}$$

which is known as the complex analytic signal associated with vector $\mathbf{F}^{(r)}(\mathbf{r},t)$. Since $\mathbf{F}^{(r)}(\mathbf{r},t)=2\mathrm{Re}[\mathbf{F}(\mathbf{r},t)]$, we can write

$$\mathbf{F}(\mathbf{r},t)=\frac{1}{2}\left[\mathbf{F}^{(r)}(\mathbf{r},t)+i\mathbf{F}^{(i)}(\mathbf{r},t)\right], \tag{3}$$

where the real and imaginary parts constitute a Hilbert transform pair. We mention that, strictly speaking, the Fourier presentation of Eq. (1) does not exist for stationary quantities, but its use can be justified by going beyond the ordinary function theory [15].

2.2 Maxwell's equations

Each realization of the electromagnetic field, either real or the complex analytic counterpart, satisfies the macroscopic Maxwell equations, which in SI units are written as

$$\nabla \cdot \mathbf{D}(\mathbf{r},t) = \rho(\mathbf{r},t), \tag{4}$$
$$\nabla \cdot \mathbf{B}(\mathbf{r},t) = 0, \tag{5}$$
$$\nabla \times \mathbf{E}(\mathbf{r},t) = -\frac{\partial \mathbf{B}(\mathbf{r},t)}{\partial t}, \tag{6}$$
$$\nabla \times \mathbf{H}(\mathbf{r},t) = \mathbf{j}(\mathbf{r},t) + \frac{\partial \mathbf{D}(\mathbf{r},t)}{\partial t}. \tag{7}$$

Here $\mathbf{E}$ and $\mathbf{H}$ are the electric and magnetic fields, respectively, and $\mathbf{D}$ is the electric displacement and $\mathbf{B}$ the magnetic induction. The quantities ρ and $\mathbf{j}$ represent the density of free charges and currents that may be present in the medium. The vectors $\mathbf{D}$ and $\mathbf{B}$ take into account the response of the medium to the electromagnetic field. They are connected to the polarization, $\mathbf{P}$, and magnetization, $\mathbf{M}$, induced in the medium by an electromagnetic field through the relations,

$$\mathbf{D}(\mathbf{r},t) = \epsilon_0 \mathbf{E}(\mathbf{r},t) + \mathbf{P}(\mathbf{r},t), \tag{8}$$
$$\mathbf{B}(\mathbf{r},t) = \mu_0 \left[\mathbf{H}(\mathbf{r},t) + \mathbf{M}(\mathbf{r},t)\right], \tag{9}$$

where the quantities ϵ_0 and μ_0 are the vacuum permittivity and permeability, respectively. Maxwell's equations completely describe the behavior of an electromagnetic field in any medium. We, however, consider fields only in homogeneous, isotropic, and linear media. In this case, the polarization and magnetization are obtained in terms of the following constitutive relations [20],

$$\mathbf{P}(\mathbf{r},t) = \frac{\epsilon_0}{2\pi} \int_{-\infty}^{t} \chi(t-t') \mathbf{E}(\mathbf{r},t') dt', \tag{10}$$
$$\mathbf{M}(\mathbf{r},t) = \frac{1}{2\pi} \int_{-\infty}^{t} \eta(t-t') \mathbf{H}(\mathbf{r},t') dt', \tag{11}$$

where $\chi(t)$ and $\eta(t)$ are scalar quantities known as the electric and magnetic susceptibilities, respectively. The convolution integrals of Eqs. (10) and (11) state that the polarization and magnetization, at time t and in point $\mathbf{r}$, depend on the values of the electric and magnetic fields at previous instants of time t'. Thus, they obey causality.

2.3 Coherence theory in space-time domain

Correlation properties of electromagnetic fields at a pair of points $(\mathbf{r}_1, t_1)$ and $(\mathbf{r}_2, t_2)$ in the space-time domain are described in terms of the coherence tensors, defined

by [15, 21]

$$\mathcal{E}_{jk}(\mathbf{r}_1,\mathbf{r}_2,\tau) = \langle E_j^*(\mathbf{r}_1,t)E_k(\mathbf{r}_2,t+\tau)\rangle, \quad (12)$$
$$\mathcal{H}_{jk}(\mathbf{r}_1,\mathbf{r}_2,\tau) = \langle H_j^*(\mathbf{r}_1,t)H_k(\mathbf{r}_2,t+\tau)\rangle, \quad (13)$$
$$\mathcal{M}_{jk}(\mathbf{r}_1,\mathbf{r}_2,\tau) = \langle E_j^*(\mathbf{r}_1,t)H_k(\mathbf{r}_2,t+\tau)\rangle, \quad (14)$$
$$\mathcal{N}_{jk}(\mathbf{r}_1,\mathbf{r}_2,\tau) = \langle H_j^*(\mathbf{r}_1,t)E_k(\mathbf{r}_2,t+\tau)\rangle. \quad (15)$$

Here the subscripts $(j,k) = (x,y,z)$ label Cartesian components of the complex realizations, $\mathbf{E}(\mathbf{r},t)$ and $\mathbf{H}(\mathbf{r},t)$, associated with the electric and magnetic field vectors, respectively. Furthermore, due to stationarity, the statistical properties of the fields depend on time only through the difference, $\tau = t_2 - t_1$. The angle brackets in Eqs. (12)–(15) denote averaging over an ensemble of all field realizations. We remark, that in every field found in nature, correlations die out rapidly in time. Such fields are also ergoding, which implies that taking the ensemble average equals averaging over time in a single realization.

The coherence tensors obey certain symmetry relations, which follow from their definitions, and in particular we have

$$\mathcal{E}_{kj}(\mathbf{r}_1,\mathbf{r}_2,\tau) = \mathcal{E}_{jk}^*(\mathbf{r}_2,\mathbf{r}_1,-\tau), \quad (16)$$
$$\mathcal{H}_{kj}(\mathbf{r}_1,\mathbf{r}_2,\tau) = \mathcal{H}_{jk}^*(\mathbf{r}_2,\mathbf{r}_1,-\tau), \quad (17)$$
$$\mathcal{M}_{kj}(\mathbf{r}_1,\mathbf{r}_2,\tau) = \mathcal{N}_{jk}^*(\mathbf{r}_2,\mathbf{r}_1,-\tau). \quad (18)$$

The propagation of the coherence tensors is governed by differential equations which follow from the fact that the field realizations obey Maxwell's equations. This also states that the elements of the coherence tensors are not independent. The coherence tensors also satisfy various non-negative definiteness conditions. More details on these issues are available in Ref. [15].

2.4 Coherence theory in space-frequency domain

In some cases it is more appropriate to analyze the fluctuating fields in the space-frequency domain rather than in the space-time domain. For example, we see from the constitutive relations of Eqs. (10) and (11) that the response of the medium to the electromagnetic field is difficult to analyze in the space-time domain.

Cross-spectral density tensors

By taking the inverse transform of Eq. (2), and applying it to the electric and magnetic field vectors one obtains the cross-spectral tensors

$$\langle \tilde{E}_j^*(\mathbf{r}_1,\omega)\tilde{E}_k(\mathbf{r}_2,\omega')\rangle = W_{jk}^{(e)}(\mathbf{r}_1,\mathbf{r}_2,\omega)\delta(\omega-\omega'), \quad (19)$$

$$\langle \tilde{H}_j^*(\mathbf{r}_1,\omega)\tilde{H}_k(\mathbf{r}_2,\omega')\rangle = W_{jk}^{(h)}(\mathbf{r}_1,\mathbf{r}_2,\omega)\delta(\omega-\omega'), \quad (20)$$

$$\langle \tilde{E}_j^*(\mathbf{r}_1,\omega)\tilde{H}_k(\mathbf{r}_2,\omega')\rangle = W_{jk}^{(m)}(\mathbf{r}_1,\mathbf{r}_2,\omega)\delta(\omega-\omega'), \quad (21)$$

$$\langle \tilde{H}_j^*(\mathbf{r}_1,\omega)\tilde{E}_k(\mathbf{r}_2,\omega')\rangle = W_{jk}^{(n)}(\mathbf{r}_1,\mathbf{r}_2,\omega)\delta(\omega-\omega'). \quad (22)$$

The tensors $W_{jk}^{(e)}$ and $W_{jk}^{(h)}$ are, respectively, known as the electric and magnetic cross-spectral density tensors, and $W_{jk}^{(m)}$ and $W_{jk}^{(n)}$ as the mixed cross-spectral density tensors. The Dirac delta function, $\delta(\omega-\omega')$, is a consequence of the stationarity, indicating that different frequency components of the field are uncorrelated. Thus, in the stationary case, the correlation properties of the field may be analyzed by focusing on a single frequency component of a polychromatic electromagnetic field only.

Properties of cross-spectral density tensors

Each cross-spectral density tensor in Eqs. (19)–(22) and the corresponding coherence tensor in Eqs. (12)–(15) form a Fourier transform pair. This is known as the (generalized) Wiener-Khintchine theorem. For example, for the electric cross-spectral density tensor and the corresponding coherence tensor this implies that,

$$W_{jk}^{(e)}(\mathbf{r}_1,\mathbf{r}_2,\omega) = \frac{1}{2\pi}\int_{-\infty}^{\infty}\mathcal{E}_{jk}(\mathbf{r}_1,\mathbf{r}_2,\tau)e^{i\omega\tau}d\tau, \qquad (\omega\geq 0) \quad (23)$$

$$\mathcal{E}_{jk}(\mathbf{r}_1,\mathbf{r}_2,\tau) = \int_0^{\infty} W_{jk}^{(e)}(\mathbf{r}_1,\mathbf{r}_2,\omega)e^{-i\omega\tau}d\omega. \quad (24)$$

The integration in Eq. (24) extends from zero to infinity due to the fact that $\mathbf{E}(\mathbf{r},t)$, and consequently also $W_{jk}^{(e)}(\mathbf{r}_1,\mathbf{r}_2,\omega)$, are complex analytic signals for which the spectral components vanish for negative frequencies.

Similarly to the correlation tensors in the space-time domain, also the cross-spectral density tensors satisfy certain symmetry relations. For example, the equation

$$W_{kj}^{(\alpha)}(\mathbf{r}_1,\mathbf{r}_2,\omega) = \Big[W_{jk}^{(\alpha)}(\mathbf{r}_2,\mathbf{r}_1,\omega)\Big]^*, \qquad \alpha=(e,h), \quad (25)$$

holds for both the electric and magnetic cross-spectral density tensors, and the equation

$$W_{kj}^{(m)}(\mathbf{r}_1,\mathbf{r}_2,\omega) = \Big[W_{jk}^{(n)}(\mathbf{r}_2,\mathbf{r}_1,\omega)\Big]^*, \quad (26)$$

for the mixed tensors. Also certain non-negative definiteness conditions apply for the cross-spectral density tensors. In particular, for the electric cross-spectral density tensor the following holds

$$\sum_{p,q=1}^{N} \sum_{j,k} a_{jp}^{*} a_{kq} W_{jk}^{(e)}(\mathbf{r}_p, \mathbf{r}_q, \omega) \geq 0, \tag{27}$$

where a_{jp} and a_{kq} are arbitrary real or complex numbers. Other conditions of this type satisfied by the cross-spectral density tensors, as well as differential equations that govern their propagation, can be found in Ref. [15]. We note, however, that the Maxwell's equations limit the number of independent elements of the cross-spectral density tensors.

The cross-spectral density tensors have a property that is often useful in their analysis. Namely, they are correlation tensors that can be expressed as an average over an ensemble of strictly monochromatic realizations all at the same frequency ω [22]. For the electric cross-spectral density tensor, the averaging is performed over an ensemble $\{\mathbf{E}(\mathbf{r}, \omega) e^{-i\omega t}\}$, and it can be explicitly written as

$$W_{jk}^{(e)}(\mathbf{r}_1, \mathbf{r}_2, \omega) = \langle E_j^{*}(\mathbf{r}_1, \omega) E_k(\mathbf{r}_2, \omega) \rangle. \tag{28}$$

Similar expressions exist also for the other cross-spectral density tensors. We should emphasize that $\mathbf{E}(\mathbf{r}, \omega)$ is not the Fourier transform of $\mathbf{E}(\mathbf{r}, t)$.

Spectral coherence matrix

By setting $\mathbf{r}_1 = \mathbf{r}_2 = \mathbf{r}$ in Eq. (28), the spectral coherence matrix (electric spectral density tensor) is obtained

$$\phi_{jk}(\mathbf{r}, \omega) = W_{jk}^{(e)}(\mathbf{r}, \omega). \tag{29}$$

The diagonal elements $\phi_{jj}(\mathbf{r}, \omega)$ $(j = x, y, z)$ are the spectral densities or, loosely speaking, intensities associated with the field component E_j at the frequency ω. Their sum, or the trace of the tensor $\phi_{jk}(\mathbf{r}, \omega)$, produces the total spectral density of the field. In addition, the off-diagonal elements, $\phi_{jk}(\mathbf{r}, \omega),\ j \neq k$, characterize the correlations between the orthogonal components of the electric field at a given point. Sometimes it is useful to normalize the off-diagonal elements of the coherence matrix by defining

$$\mu_{jk}(\mathbf{r}, \omega) = \frac{\phi_{jk}(\mathbf{r}, \omega)}{\left[\phi_{jj}(\mathbf{r}, \omega)\right]^{1/2} \left[\phi_{kk}(\mathbf{r}, \omega)\right]^{1/2}}, \qquad \mu_{kj}(\mathbf{r}, \omega) = \mu_{jk}^{*}(\mathbf{r}, \omega). \tag{30}$$

The absolute value $|\mu_{jk}(\mathbf{r}, \omega)|$ is bounded between 0 and 1 and gives a measure for the degree of correlation between the two orthogonal components of the electric

field. Furthermore, the spectral coherence matrix has certain mathematical properties that are in order to be mentioned here. Firstly, it follows from Eq. (25) that the cross-spectral density tensor is Hermitian, i.e. $\phi_{jk}(\mathbf{r},\omega) = \phi^*_{kj}(\mathbf{r},\omega)$. Secondly, Eq. (27) implies that it is also non-negative definite, i.e. $\sum_{jk} a_j a_k \phi_{jk}(\mathbf{r},\omega) \geq 0$. The Hermiticity and non-negative definiteness state that the eigenvalues of the spectral coherence matrix are real and non-negative. The spectral coherence matrix is an object that contains all information about the polarization state of a fluctuating electromagnetic field in a point; the propagation properties are contained in the cross-spectral density tensors.

2.5 Remark on notations

In this section the quantities are expressed in tensorial notation, i.e., by writing down a single element of the tensor using two subscripts j and k to specify the element. This convention is standard in the coherence theory, and it is perhaps the notation that the readers are most familiar with. However, in several central publications related to the subject matter investigated in this thesis, dyadic notation is employed, and therefore, it is frequently used here, too. For example, instead of writing

$$W^{(e)}_{jk}(\mathbf{r}_1,\mathbf{r}_2,\omega) = \langle E^*_j(\mathbf{r}_1,\omega) E_k(\mathbf{r}_2,\omega)\rangle, \tag{31}$$

we write

$$\overleftrightarrow{W}_{ee}(\mathbf{r}_1,\mathbf{r}_2,\omega) = \langle \mathbf{E}^*(\mathbf{r}_1,\omega)\mathbf{E}(\mathbf{r}_2,\omega)\rangle. \tag{32}$$

When one calculates the scalar or vector product of a dyadic with a vector (or another dyadic), either from the left or right, the operation is, respectively, directed to the vector on the left or on the right in the dyadic.

3 Evanescent and Propagating Part of the Electromagnetic Field

The electromagnetic field emitted or scattered by an object always consists of both evanescent and propagating waves. The evanescent waves are bound close to the source, being significant only within a distance of wavelength from it, whereas the propagating waves can be observed in the far zone. It is known that the evanescent waves contain information about the sub-wavelength scale details of the source, though the question of how the information is stored in the evanescent field is rather complicated. Useful insight into the subject matter is gained by considering the most elementary source of electromagnetic field, i.e., the point-dipole source, and decomposing the associated free-space Green tensor into its evanescent and propagating constituents; an issue that has thoroughly been discussed in the recent literature [23–34].

The decomposition of the scalar free-space Green function, and particularly the far-zone contributions of its evanescent and propagating parts, was analyzed already in the seventies [35, 36]. It was demonstrated that in the far zone, the propagating field in every direction falls off as r^{-1} with the distance r from the source, and that the evanescent field falls off as $r^{-3/2}$, except for two special directions where it decays as r^{-1}. These results indicate that the propagating field completely overwhelms the evanescent field in the far zone, apart from the two particular directions which are fixed by the angular-spectrum construction of the field. Expressions in terms of Bessel and Lommel functions have been derived for both the evanescent and propagating parts of the Green function [37].

Surprisingly, in view of the known results of the scalar investigations, a few years ago a decomposition of the Green tensor, yielding comparable far-zone contributions of the evanescent and propagating electromagnetic fields emerged in the literature and was then extensively used in the analysis of scanning near-field optical microscopy [38–47]. This result was criticized in several publications; by Wolf and Foley using scalar theory [23], by us using electromagnetic theory [Paper I], and then by several other authors [24–30], who all confuted the claims put forward in Refs. [38–47]. In Paper I, we explicitly pointed out the mistakes of Refs. [38–47], and provided the correct forms for both the evanescent and propagating parts of the free-space Green tensor, which are valid throughout the space, and which are suitable for the numerical analysis of optical near fields. Also another decomposition of the Green tensor was put forward by the same author [47–49], which likewise leads to equal contributions of the evanescent and propagating fields in the far zone. This result was pointed out to be incorrect in Ref. [34]. Discussion about the subject matter has been active, and it continues to attract interest as evidenced by the recent

investigations by Berry [31] and by Arnoldus and Foley [32, 33].

In this section, as an introduction to the treatment of optical near fields, we derive an angular-spectrum representation for the free-space Green tensor, which expresses the point-dipole field in terms of the evanescent and propagating electromagnetic plane waves. We also outline the decomposition of the field into its evanescent and propagating parts, and briefly discuss their far-zone behavior. In the following, we deal with fully deterministic fields, though the extension of the results to cover also fluctuating fields is straightforward [15].

3.1 Dipole field

The field at $\mathbf{r}$ produced by a current dipole at $\mathbf{r}'$ in vacuum is given by the expression

$$\mathbf{E}(\mathbf{r},\omega) = i\mu_0\omega \overleftrightarrow{G}(\mathbf{r}-\mathbf{r}',\omega)\cdot\mathbf{j}(\mathbf{r}',\omega), \tag{33}$$

where

$$\overleftrightarrow{G}(\mathbf{r}-\mathbf{r}',\omega) = \left(\overleftrightarrow{U} + \frac{1}{k_0^2}\nabla_{\mathbf{r}}\nabla_{\mathbf{r}}\right) G(\mathbf{r}-\mathbf{r}',\omega) \tag{34}$$

is the free-space Green tensor [50], which contains all information about the field components created by the point source. Here $\overleftrightarrow{U}$ is the unit tensor, and $G(\mathbf{r}-\mathbf{r}',\omega)$ is the (scalar) free-space Green function, given by

$$G(\mathbf{r}-\mathbf{r}',\omega) = \frac{e^{ik_0|\mathbf{r}-\mathbf{r}'|}}{4\pi|\mathbf{r}-\mathbf{r}'|}, \tag{35}$$

and representing the spherical wave expanding from the point $\mathbf{r}'$.

3.2 Plane-wave representation of the Green tensor

For simplicity we assume that the point source is in the origin and set $\mathbf{r}' = 0$. The Weyl expansion is a half-space representation for the spherical wave that contains both evanescent and propagating plane waves [15]. For the half-spaces $z > 0$ and $z < 0$, this is written as

$$G(\mathbf{r},\omega) = \frac{ik_0}{8\pi^2}\iint_{-\infty}^{\infty}\frac{1}{u_z}e^{ik_0\hat{u}_\pm\cdot\mathbf{r}}du_x du_y, \tag{36}$$

where $\hat{u}_\pm = u_x\hat{u}_x + u_y\hat{u}_y \pm u_z\hat{u}_z$, with the upper and lower signs referring to the half-spaces $z > 0$ and $z < 0$, respectively. Furthermore,

$$\begin{cases} u_z = +\sqrt{1-u_x^2-u_y^2}, & \text{when } u_x^2+u_y^2 \le 1 \\ u_z = +i\sqrt{u_x^2+u_y^2-1}, & \text{when } u_x^2+u_y^2 > 1, \end{cases} \tag{37}$$

indicating that for $u_x^2 + u_y^2 \leq 1$ the plane waves propagate in the direction specified by $\hat{u}_\pm$, and for $u_x^2 + u_y^2 > 1$ their amplitudes decay exponentially with distance from the plane $z = 0$.

Inserting the scalar plane-wave expression of Eq. (36) into Eq. (34), one obtains

$$\overleftrightarrow{G}(\mathbf{r},\omega) = \frac{ik_0}{8\pi^2}\int\!\!\int_{-\infty}^{\infty} \frac{1}{u_z}\left[\overleftrightarrow{U} - \hat{u}_\pm\hat{u}_\pm\right] e^{ik_0\hat{u}_\pm\cdot\mathbf{r}}du_x du_y. \tag{38}$$

This expression may be developed further by constructing two orthonormal right-handed vector triads $(\hat{u}_+, \hat{p}_+, \hat{s})$ and $(\hat{u}_-, \hat{p}_-, \hat{s})$, using definitions $\hat{s} = \hat{u}_\pm \times \hat{u}_z/|\hat{u}_\pm \times \hat{u}_z|$, and $\hat{p}_\pm = \hat{s}\times\hat{u}_\pm$ (see Fig. 1). These definitions hold even though the vectors $\hat{u}_\pm$ and $\hat{p}_\pm$ are complex for the evanescent waves. The unit vectors $\hat{s}$ and $\hat{p}_\pm$ correspond to the s- and p-polarization vectors of plane waves. Since $\overleftrightarrow{U} = \hat{s}\hat{s} + \hat{p}_\pm\hat{p}_\pm + \hat{u}_\pm\hat{u}_\pm$, Eq. (38) can be rewritten as

$$\overleftrightarrow{G}\,(\mathbf{r},\omega) = \frac{ik_0}{8\pi^2}\int\!\!\int_{-\infty}^{\infty} \frac{1}{u_z}\left[\hat{s}\hat{s} + \hat{p}_\pm\hat{p}_\pm\right] e^{ik_0\hat{u}_\pm\cdot\mathbf{r}}du_x du_y. \tag{39}$$

This equation provides an intuitive expression for the free-space Green tensor that is analogous to the Weyl expansion in the scalar case, Eq. (36). Substituting Eq. (39) in the dipole-field expression, Eq. (33), we obtain an expression for the field in terms of plane waves which are explicitly represented by their s- and p-polarized components. Formula (39) is particularly useful in constructing Green tensors for more complicated geometries involving, for instance, multilayers [51].

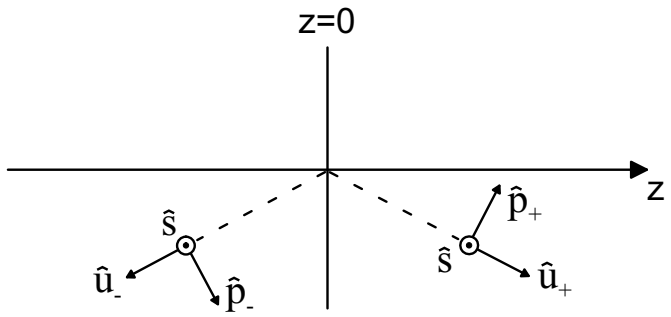

Figure 1: Illustration of the vector triads $(\hat{u}_\pm, \hat{p}_\pm, \hat{s})$ when the vectors are real.

3.3 Evanescent and propagating part of the Green tensor

The tensor of Eq. (39) can be decomposed into a sum of two integrals

$$\overleftrightarrow{G}(\mathbf{r},\omega) = \overleftrightarrow{G}_H(\mathbf{r},\omega) + \overleftrightarrow{G}_E(\mathbf{r},\omega), \tag{40}$$

where

$$\overleftrightarrow{G}_H(\mathbf{r},\omega) = \frac{ik_0}{8\pi^2}\iint_{u_x^2+u_y^2\le 1}\frac{1}{u_z}\left[\hat{s}\hat{s}+\hat{p}_\pm\hat{p}_\pm\right]e^{ik_0\hat{u}_\pm\cdot\mathbf{r}}du_x du_y, \tag{41}$$

and

$$\overleftrightarrow{G}_E(\mathbf{r},\omega) = \frac{ik_0}{8\pi^2}\iint_{u_x^2+u_y^2>1}\frac{1}{u_z}\left[\hat{s}\hat{s}+\hat{p}_\pm\hat{p}_\pm\right]e^{ik_0\hat{u}_\pm\cdot\mathbf{r}}du_x du_y. \tag{42}$$

The tensor $\overleftrightarrow{G}_H(\mathbf{r},\omega)$ contains all the propagating plane waves and is therefore called the propagating or homogeneous part. Similarly, the tensor $\overleftrightarrow{G}_E(\mathbf{r},\omega)$ contains all the exponentially decaying plane waves and is called the evanescent or inhomogeneous part. For brevity, we consider only the evanescent part, but keep in mind that the propagating part is obtained from the relation $\overleftrightarrow{G}_H(z,\omega) = \overleftrightarrow{G}(z,\omega) - \overleftrightarrow{G}_E(z,\omega)$. An expression for the evanescent part of the Green tensor where one of the integrations has been carried out, and which is valid at any distance from the source, is derived in Paper I. It is explicitly written as

$$\overleftrightarrow{G}_E(\mathbf{r},\omega) = \frac{k_0}{4\pi}\begin{pmatrix} I_0^E + \frac{k_0^2(x^2-y^2)}{\beta^3}L_1^E - \frac{k_0^2x^2}{\beta^2}L_2^E & \frac{k_0^2xy}{\beta^2}\left[\frac{2}{\beta}L_1^E - L_2^E\right] & \pm\frac{k_0x}{\beta}L_3^E \\ \frac{k_0^2xy}{\beta^2}\left[\frac{2}{\beta}L_1^E - L_2^E\right] & I_0^E + \frac{k_0^2(y^2-x^2)}{\beta^3}L_1^E - \frac{k_0^2y^2}{\beta^2}L_2^E & \pm\frac{k_0y}{\beta}L_3^E \\ \pm\frac{k_0x}{\beta}L_3^E & \pm\frac{k_0y}{\beta}L_3^E & L_2^E \end{pmatrix}, \tag{43}$$

where

$$\begin{cases} L_1^E(\mathbf{r}) = \frac{1}{\alpha}[J_1(\beta) + \beta I_1^E], \\ L_2^E(\mathbf{r}) = I_0^E + I_2^E, \\ L_3^E(\mathbf{r}) = \frac{1}{\beta}[J_0(\beta) - \alpha I_0^E + 2I_1^E - \alpha I_2^E], \end{cases} \tag{44}$$

and

$$I_m^E(\mathbf{r}) = \int_0^\infty v^m e^{-\alpha(z)v}J_0\left[\beta(x,y)\sqrt{v^2+1}\right]dv. \tag{45}$$

In these equations J_0 and J_1 are Bessel functions and the coordinate-dependent parameters $\alpha(z)$ and $\beta(x,y)$ have the form

$$\alpha(z) = k_0|z|, \tag{46}$$

$$\beta(x,y) = k_0\sqrt{x^2+y^2}. \tag{47}$$

It appears that there exists no closed-form expression for the evanescent (and propagating) part, except for the direction of the z axis and in the $z = 0$ plane. Along the z axis the evanescent part takes the form

$$\overleftrightarrow{G}_E(z,\omega) = \left(\frac{1}{2|z|} - \frac{1}{k_0^2|z|^3}\right)\overleftrightarrow{U} + \left(\frac{1}{2|z|} + \frac{3}{k_0^2|z|^3}\right)\hat{u}_z\hat{u}_z, \tag{48}$$

whereas in the $z = 0$ plane $\overleftrightarrow{G}_E(\mathbf{r},\omega)$ is obtained by inserting into Eq. (43) the relations

$$\begin{cases} I_0^E(z=0) = \frac{\cos\beta}{\beta}, \\ I_1^E(z=0) = -\frac{J_1(\beta)}{\beta}, \\ I_2^E(z=0) = -\frac{\sin\beta}{\beta^2} - \frac{\cos\beta}{\beta^3}. \end{cases} \tag{49}$$

and

$$\begin{cases} L_1^E(z=0) = \frac{\sin\beta}{\beta} + \frac{\cos\beta}{\beta^2}, \\ L_2^E(z=0) = \frac{\cos\beta}{\beta} - \frac{\sin\beta}{\beta^2} - \frac{\cos\beta}{\beta^3}, \\ L_3^E(z=0) = -\frac{J_2(\beta)}{\beta}. \end{cases} \tag{50}$$

The results of Eqs. (48)–(50) indicate that in the z axis and in the $z = 0$ plane the evanescent contribution falls off as r^{-1} in the far zone. Thus, in these two special directions the evanescent and propagating contributions are comparable. In any other direction the far-zone contribution of the evanescent field is obtained by inserting into Eq. (34) the asymptotic expression for the evanescent part of the scalar spherical wave [15, 20, 35, 36]. Doing so, one finds that the evanescent part of the free-space Green tensor decays as $r^{-3/2}$. This implies that the propagating part, which falls off as r^{-1}, for $r \gg \lambda$, completely overwhelms the evanescent contribution in the far zone, except for the two special directions.

It is important to note that when writing the Weyl expression of Eq. (36), the whole space is divided into two source-free half-spaces separated by the plane $z = 0$. For a point source this division is quite arbitrary and could equally well be made using any other plane. Each choice of the dividing plane will, however, lead to different mathematical values for the propagating and evanescent parts of the field in a given point of space. In all cases the evanescent plane waves will decay exponentially in the direction normal to the dividing plane and they will propagate in directions parallel to that plane. Since all the different choices of orientation of the dividing plane must be considered as correct, the physical meaning of the decomposition of the spherical-wave into its propagating and evanescent parts is somewhat vague. The decomposition should be understood simply as a mathematical tool, which becomes meaningful only when applied to a real physical situation in which the geometry of the problem fixes the orientation of the dividing plane. In any case, one should remember that in a near-field measurement, the detected signal is always due to the total field, rather than the evanescent field only.

4 Polarization of Random Electromagnetic Fields

Theoretical means to analyze the partial polarization of planar quasimonochromatic wave fields in terms of the 2×2 equal-time coherence-matrix or the Stokes parameters, was introduced by Wolf over 40 years ago [52]. He proved that for any planar field, the 2×2 coherence matrix can be uniquely decomposed into a sum of two matrices, one corresponding to a fully unpolarized and the other to a fully polarized field. This finding led to the introduction of the concept of degree of polarization for 2D (two-dimensional) electromagnetic fields, defined as the ratio of the intensity contained in the polarized part to that of the total field. He also pointed out that the 2D degree of polarization is a measure for the degree of correlation that exists between the two orthogonal field components. Furthermore, Wolf demonstrated that the degree of polarization of a field can be measured by a simple experiment involving a compensator and a polarizer. Since then the degree of polarization has taken its place as a central parameter in characterizing the polarization state of fluctuating fields [15–19]. It has been extensively used in various polarization studies dealing with planar fields, such as uniform, well-collimated optical beams [53] or radiated wide-angle far fields [54, 55], which locally behave as plane waves.

The original treatment of the partial polarization of the electromagnetic field is restricted only to 2D quasi-monochromatic fields. Although the formalism can be extended to include wide-bandwidth light by performing the analysis in the space-frequency domain, little attention has been paid to the question whether the formalism could be extended to cover arbitrary 3D (three-dimensional) fields, which may have non-planar wave fronts. Such a theory would evidently be valuable in near-field optics and in investigations of high numerical aperture imaging systems, for example. The formulation of the 3D degree of polarization did, in fact, already attract some interest in the seventies and early eighties in the works by Samson *et al.* on geophysics [56–58], and by Barakat on optical fields [59, 60]. It seems that Samson and Barakat were unaware of each other's works, probably due to the fact their investigations belong to rather different contexts. In Ref. [56] Samson approaches the problem by investigating different expansions of the full 3×3 spectral coherence matrix. For one such expansion, he interprets the expansion coefficients as the nine spectral Stokes parameters and defines the 3D degree of polarization in a manner analogous to the 2D Stokes parameter expression. Much of the same was also performed by Barakat in Ref. [59]. In congruence, the authors of Refs. [57, 58, 60] formulate the 3D degree of polarization in terms of scalar invariants, which are traces of different powers of the spectral coherence matrix and its determinant. These invariants appear as coefficients in the characteristic equation of the coherence matrix. Based on such a treatment Barakat, as a matter of fact, proposes in Ref. [60] two measures for the degree of polarization, of which one is the same as that suggested

by Samson. More recently, the polarization of 3D electromagnetic fields has been examined by Brosseau [19, 61, 62] in terms of polarization entropy, and by Carozzi *et al.* [63] in terms of Stokes parameters, though the latter work concentrates on fully polarized fields only. However, in any of these investigations no physical interpretation for the 3D degree of polarization is provided. This is, perhaps, due to the fact that, unlike in the 2D case, the 3×3 coherence matrix cannot, in general, be decomposed into the sum of matrices describing fully polarized and fully unpolarized fields. In Paper II, we demonstrate that the 3D degree of polarization is a measure for the average degree of correlation that exists between the three orthogonal electric field components. This brings along a physical meaning for the 3D degree of polarization that is analogous to the interpretation of the concept in 2D. Moreover, in Paper II we point out an important difference between the 2D and 3D descriptions; the value of the degree of polarization, in general, depends on the dimensionality of the treatment.

In this Chapter, we first recall the conventional 2D description of partial polarization, both the 2×2 coherence-matrix treatment and the Stokes parametrization of the field, and then review the new formalism based on the full 3×3 coherence matrix that covers fields with arbitrary wave structures [Paper II]. Then as an example, the 3D formalism is applied to analyze the degree of polarization in optical near fields emitted by thermal half-space sources, particulary in cases where the near field is strongly polarized due to resonant surface waves such as surface plasmon or phonon polaritons [Paper III]. This work is the first study ever to assess the partial polarization of optical near fields. The chapter ends with an analysis of the partial polarization of statistically homogeneous free electromagnetic fields [Paper IV].

4.1 Degree of polarization for planar fields

We begin by outlining the conventional 2D theory for the degree of polarization. More comprehensive overview with mathematical details can be found in Paper II, or in many textbooks on coherence theory [15–19].

Coherence-matrix treatment

We consider a planar electromagnetic field propagating in the z direction with the electric field oscillating in the xy plane (see Fig. 2). Since the electric field oscillation is restricted to a plane, it is adequate to describe the polarization statistics by the 2×2 spectral coherence matrix, $\Phi_2(\mathbf{r}, \omega)$, associated with the x and y components of the field. In the matrix form, $\Phi_2(\mathbf{r}, \omega)$ is written as

$$\Phi_2(\mathbf{r}, \omega) = \begin{pmatrix} \phi_{xx}(\mathbf{r}, \omega) & \phi_{xy}(\mathbf{r}, \omega) \\ \phi_{yx}(\mathbf{r}, \omega) & \phi_{yy}(\mathbf{r}, \omega) \end{pmatrix}, \tag{51}$$

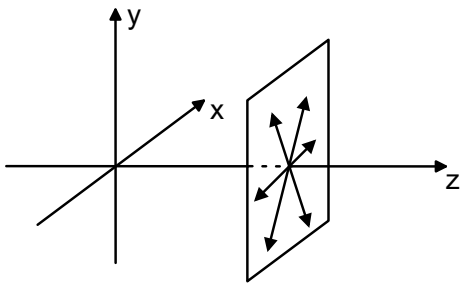

Figure 2: Illustration of a plane wave propagating in the z direction with the electric field oscillating in the xy plane.

with the elements defined in Eq. (29). The coherence matrix in Eq. (51) can be uniquely decomposed into a sum of two matrices, one corresponding to fully polarized light and the other to fully unpolarized light. The degree of polarization of the field can then be expressed as the ratio of the intensity of the polarized part to the total intensity of the field. The resulting expression for the degree of polarization of the two-dimensional field, $P_2(\mathbf{r},\omega)$, has the form

$$P_2^2(\mathbf{r},\omega) = 1 - \frac{4\det\left[\Phi_2(\mathbf{r},\omega)\right]}{\mathrm{tr}^2\left[\Phi_2(\mathbf{r},\omega)\right]} = 2\left\{\frac{\mathrm{tr}\left[\Phi_2^2(\mathbf{r},\omega)\right]}{\mathrm{tr}^2\left[\Phi_2(\mathbf{r},\omega)\right]} - \frac{1}{2}\right\}. \tag{52}$$

This quantity is bounded to the interval $0 \leq P_2(\mathbf{r},\omega) \leq 1$, with the values $P_2(\mathbf{r},\omega) = 0$ and $P_2(\mathbf{r},\omega) = 1$ corresponding to a completely unpolarized and polarized plane wave, respectively. We see at once that the result is invariant under unitary transformations, and thus also under rotations, since trace and determinant are scalar invariants under such operations. Due to Hermiticity, the coherence matrix can always be diagonalized by a unitary transformation, and we can readily express the degree of polarization in terms of the eigenvalues $A_1(\mathbf{r},\omega)$ and $A_2(\mathbf{r},\omega)$ of the matrix

$$P_2(\mathbf{r},\omega) = \left|\frac{A_1(\mathbf{r},\omega) - A_2(\mathbf{r},\omega)}{A_1(\mathbf{r},\omega) + A_2(\mathbf{r},\omega)}\right|. \tag{53}$$

Stokes-parameter representation

An alternative description of the 2D degree of polarization can be based on the Stokes parameters. The 2D Stokes parameters $S_j(\mathbf{r},\omega),\ (j = 0\ldots3)$ are measurable quantities that appear as expansion coefficients when the coherence matrix is expanded in terms of the 2×2 unit matrix σ_0 and the three Pauli matrices, or generators of the SU(2) symmetry group, $\sigma_j\ (j = 1\ldots3)$, i.e.,

$$\Phi_2(\mathbf{r},\omega) = \frac{1}{2}\sum_{j=0}^{3} S_j(\mathbf{r},\omega)\sigma_j, \tag{54}$$

where

$$\begin{cases} S_0(\mathbf{r},\omega) = \phi_{xx}(\mathbf{r},\omega) + \phi_{yy}(\mathbf{r},\omega), \\ S_1(\mathbf{r},\omega) = \phi_{xx}(\mathbf{r},\omega) - \phi_{yy}(\mathbf{r},\omega), \\ S_2(\mathbf{r},\omega) = \phi_{xy}(\mathbf{r},\omega) + \phi_{yx}(\mathbf{r},\omega), \\ S_3(\mathbf{r},\omega) = i\left[\phi_{yx}(\mathbf{r},\omega) - \phi_{xy}(\mathbf{r},\omega)\right]. \end{cases} \tag{55}$$

We see that the first Stokes parameter $S_0(\mathbf{r},\omega)$ is proportional to the spectral density of the field. The parameter $S_1(\mathbf{r},\omega)$ describes the excess in spectral density of the x component over that of the y component of the field. The parameter $S_2(\mathbf{r},\omega)$ represents the excess of $+45^\circ$ linearly polarized component over -45° linearly polarized component, and $S_3(\mathbf{r},\omega)$ the excess in the spectral density of the right-hand circularly polarized field component over the left-hand circularly polarized one [16, 19].

In terms of the Stokes parameters the degree of polarization of Eq. (52) takes on the form

$$P_2(\mathbf{r},\omega) = \frac{\left[S_1^2(\mathbf{r},\omega) + S_2^2(\mathbf{r},\omega) + S_3^2(\mathbf{r},\omega)\right]^{1/2}}{S_0(\mathbf{r},\omega)}. \tag{56}$$

When the field is fully polarized, the polarization state can be geometrically represented as a point $(S_1(\mathbf{r},\omega), S_2(\mathbf{r},\omega), S_3(\mathbf{r},\omega))$ on a sphere of radius $S_0(\mathbf{r},\omega)$, the so-called Poincaré sphere. This is illustrated in Fig. 3. The equator of the sphere corresponds to linearly polarized light, and the north and south poles to right-hand and left-hand circularly polarized light, respectively. In the origin of the Poincaré sphere the field is fully unpolarized and in every other inner point partially polarized.

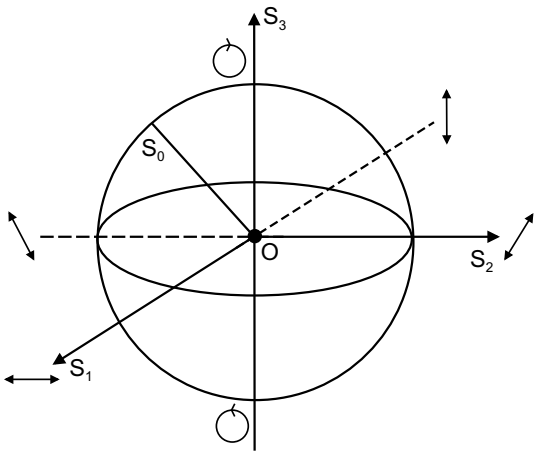

Figure 3: The Poincaré sphere for representing the polarization state of a planar field.

Finally, we note that the 2D degree of polarization is closely related to the degree of correlation, defined in Eq. (30). As was already pointed out, the value of the 2D degree of polarization does not depend on the orientation of the orthogonal two-dimensional coordinate system in the plane perpendicular to the wave's propagation direction, but the degree of correlation does. One can show that

$$P_2(\mathbf{r},\omega) \geq |\mu_{xy}(\mathbf{r},\omega)|, \tag{57}$$

which states that the maximum value of the degree of correlation is equal to the degree of polarization of the wave. The equality holds in a coordinate system in which the intensities in the x and y directions are equal, i.e., $\phi_{xx}(\mathbf{r},\omega) = \phi_{yy}(\mathbf{r},\omega)$. This situation can always be achieved by a suitable rotation of the coordinate system [16, 52].

4.2 Degree of polarization for non-planar fields

We now focus on the problem of how the treatment of the two-dimensional fields could be extended to include arbitrary electromagnetic fields in which the oscillations take place in three dimensions (see Fig. 4). The following presentation with more mathematical details can be found in Paper II.

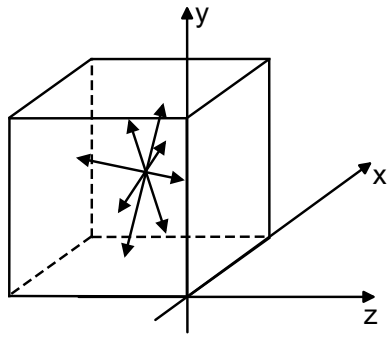

Figure 4: Illustration of the field with oscillations taking place in three dimensions.

Stokes-parameter representation

We proceed analogously to the 2D case, and expand the 3×3 spectral coherence matrix,

$$\Phi_3(\mathbf{r},\omega) = \begin{pmatrix} \phi_{xx}(\mathbf{r},\omega) & \phi_{xy}(\mathbf{r},\omega) & \phi_{xz}(\mathbf{r},\omega) \\ \phi_{yx}(\mathbf{r},\omega) & \phi_{yy}(\mathbf{r},\omega) & \phi_{yz}(\mathbf{r},\omega) \\ \phi_{zx}(\mathbf{r},\omega) & \phi_{zy}(\mathbf{r},\omega) & \phi_{zz}(\mathbf{r},\omega) \end{pmatrix}, \tag{58}$$

with the elements given in Eq. (29), in the form [19, 56]

$$\Phi_3(\mathbf{r},\omega) = \frac{1}{3}\sum_{j=0}^{8}\Lambda_j(\mathbf{r},\omega)\lambda_j. \tag{59}$$

In Eq. (59), λ_0 is the 3×3 unit matrix and the matrices $\lambda_j, (j = 1\ldots 8)$ are the Gell-Mann matrices [65] or the eight generators of the SU(3) symmetry group. The basis matrices are Hermitian, trace orthogonal and linearly independent. The expansion coefficients $\Lambda_k(\mathbf{r},\omega)$ in Eq. (59) are explicitly written as,

$$\begin{cases} \Lambda_0(\mathbf{r},\omega) = \phi_{xx}(\mathbf{r},\omega) + \phi_{yy}(\mathbf{r},\omega) + \phi_{zz}(\mathbf{r},\omega), \\ \Lambda_1(\mathbf{r},\omega) = \frac{3}{2}\left[\phi_{xy}(\mathbf{r},\omega) + \phi_{yx}(\mathbf{r},\omega)\right], \\ \Lambda_2(\mathbf{r},\omega) = \frac{3}{2}i\left[\phi_{xy}(\mathbf{r},\omega) - \phi_{yx}(\mathbf{r},\omega)\right], \\ \Lambda_3(\mathbf{r},\omega) = \frac{3}{2}\left[\phi_{xx}(\mathbf{r},\omega) - \phi_{yy}(\mathbf{r},\omega)\right], \\ \Lambda_4(\mathbf{r},\omega) = \frac{3}{2}\left[\phi_{xz}(\mathbf{r},\omega) + \phi_{zx}(\mathbf{r},\omega)\right], \\ \Lambda_5(\mathbf{r},\omega) = \frac{3}{2}i\left[\phi_{xz}(\mathbf{r},\omega) - \phi_{zx}(\mathbf{r},\omega)\right], \\ \Lambda_6(\mathbf{r},\omega) = \frac{3}{2}\left[\phi_{yz}(\mathbf{r},\omega) + \phi_{zy}(\mathbf{r},\omega)\right], \\ \Lambda_7(\mathbf{r},\omega) = \frac{3}{2}i\left[\phi_{yz}(\mathbf{r},\omega) - \phi_{zy}(\mathbf{r},\omega)\right], \\ \Lambda_8(\mathbf{r},\omega) = \frac{\sqrt{3}}{2}\left[\phi_{xx}(\mathbf{r},\omega) + \phi_{yy}(\mathbf{r},\omega) - 2\phi_{zz}(\mathbf{r},\omega)\right]. \end{cases} \tag{60}$$

We see that the expansion coefficients are analogous to those of the 2D formalism, and thus we call them the 3D (spectral) Stokes parameters. As in the 2D formalism, the first Stokes parameter is proportional to the total spectral density of the field. Moreover, we may interpret the parameters $\Lambda_1(\mathbf{r},\omega)$ and $\Lambda_2(\mathbf{r},\omega)$ as playing a role analogous to the parameters $S_2(\mathbf{r},\omega)$ and $S_3(\mathbf{r},\omega)$ in the 2D formalism. The same interpretation also holds for the pairs $[\Lambda_4(\mathbf{r},\omega), \Lambda_5(\mathbf{r},\omega)]$ and $[\Lambda_6(\mathbf{r},\omega), \Lambda_7(\mathbf{r},\omega)]$, but in the xz and yz planes, respectively. The parameter $\Lambda_3(\mathbf{r},\omega)$ is obviously analogous to $S_1(\mathbf{r},\omega)$, and $\Lambda_8(\mathbf{r},\omega)$ represents the sum of the excess in spectral density in the x and y directions over that in the z direction.

Three-dimensional degree of polarization

The 3D degree of polarization, $P_3(\mathbf{r},\omega)$, can be expressed in terms of the 3D Stokes parameters in the form

$$P_3^2(\mathbf{r},\omega) = \frac{1}{3}\frac{\sum_{j=1}^{8}\Lambda_j^2(\mathbf{r},\omega)}{\Lambda_0^2(\mathbf{r},\omega)}. \tag{61}$$

This form is analogous to Eq. (56), and it has previously been put forward by Samson [56] and Barakat [59]. On substituting the Stokes parameters of Eq. (60) into

Eq. (61), the 3D degree of polarization can be expressed in terms of the 3×3 coherence matrix as

$$P_3^2(\mathbf{r},\omega) = \frac{3}{2}\left\{\frac{\mathrm{tr}\left[\Phi_3^2(\mathbf{r},\omega)\right]}{\mathrm{tr}^2\left[\Phi_3(\mathbf{r},\omega)\right]} - \frac{1}{3}\right\}. \tag{62}$$

It is straightforward to verify that this quantity is bounded between $0 \leq P_3(\mathbf{r},\omega) \leq 1$ [Paper II]. Moreover, we see that Eq. (62) is invariant under unitary transformations and, consequently, the value of the 3D degree of polarization is independent of the orientation of the orthogonal coordinate system. Due to the Hermiticity, we may diagonalize the coherence matrix and express the 3D degree of polarization in the form

$$P_3^2(\mathbf{r},\omega) = \frac{\frac{1}{2}\sum_{i,j=1}^{3}\left[A_i(\mathbf{r},\omega) - A_j(\mathbf{r},\omega)\right]^2}{\left[A_1(\mathbf{r},\omega) + A_2(\mathbf{r},\omega) + A_3(\mathbf{r},\omega)\right]^2}, \tag{63}$$

where $A_i(\mathbf{r},\omega)$, $i = (1,2,3)$, are the (real and non-negative) eigenvalues of the coherence matrix.

The physical meaning of the expression for the 3D degree of polarization can be established by considering its relation to the degrees of correlation between the orthogonal field components. One can show that the following inequality holds [Paper II]

$$P_3^2(\mathbf{r},\omega) \geq \frac{\sum_{ij}|\mu_{ij}(\mathbf{r},\omega)|^2\phi_{ii}(\mathbf{r},\omega)\phi_{jj}(\mathbf{r},\omega)}{\sum_{ij}\phi_{ii}(\mathbf{r},\omega)\phi_{jj}(\mathbf{r},\omega)}, \tag{64}$$

where the summation is performed over the pairs $(ij) = (xy, xz, yz)$. Equation (64) states that the square of the 3D degree of polarization sets the upper limit to the average of the squared correlations weighted by the corresponding spectral densities (cf. Eq. (57)). We note that the value of the right-hand side of Eq. (64) depends on the orientation of the coordinate system, but the left-hand side does not. The right-hand side reaches the value $P_3^2(\mathbf{r},\omega)$ if the coordinate system is oriented in such a way that $\phi_{xx}(\mathbf{r},\omega) = \phi_{yy}(\mathbf{r},\omega) = \phi_{zz}(\mathbf{r},\omega)$. Such an orientation can always be found. In this case, the equality sign holds and we obtain

$$P_3^2(\mathbf{r},\omega) = \frac{|\mu_{xy}(\mathbf{r},\omega)|^2 + |\mu_{xz}(\mathbf{r},\omega)|^2 + |\mu_{yz}(\mathbf{r},\omega)|^2}{3}, \tag{65}$$

indicating that the square of the 3D degree of polarization is equal to the pure average of the squared correlations prevailing between the three orthogonal electric field components in this specific coordinate system. This result is analogous to Eq. (57) of the 2D case, and it agrees well with an intuitive physical picture of the degree of polarization.

We remark that the expression of Eq. (61) suggests that in analogy with the three-dimensional Poincaré sphere, it is, in principle, possible to characterize the polarization state of a 3D electromagnetic field in terms of a sphere in the eight-dimensional

Stokes-parameter space. However, one should keep in mind that the coherence matrix represents a solution to the Maxwell's equations, although in a single point, and therefore the Stokes parameters cannot, in general, be independent. Thus, for a given field, only a portion of the sphere would be accessible. However, owing to the large number of dimensions, the Poincaré sphere construction would not provide much physical (or geometrical) intuition to the subject.

4.3 Differences between the 2D and 3D formalisms

It is straightforward to show that the two- and three-dimensional formalisms do not, in general, produce the same value for the degree of polarization. For example, for plane waves the 3D degree of polarization is always bounded in the interval [Paper II]

$$\frac{1}{2} \leq P_3(\mathbf{r},\omega) \leq 1, \tag{66}$$

where the lowest value, $P_3(\mathbf{r},\omega) = 1/2$, corresponds to a plane wave, which in the 2D sense is fully unpolarized. Thus, a planar field cannot be fully unpolarized in the 3D formalism. This is as expected, since in such a field the oscillations are restricted to a single plane, and consequently, when treated as three-dimensional the field cannot have a zero degree of polarization. Furthermore, the range of values $0 \leq P_3(\mathbf{r},\omega) < 1/2$ is accessed only by 3D fields with weak correlations between the field components. The lowest value, $P_3(\mathbf{r},\omega) = 0$, corresponds to the case in which the intensities of the three orthogonal components are the same and no correlations exist between any pairs of the electric field components. This is mathematically expressed as $\Phi_3(\mathbf{r},\omega) \propto \overleftrightarrow{U}$.

The most intuitive understanding of the differences between the 2D and 3D formalisms is perhaps obtained by considering Fig. 5. In the upper part of the figure an unpolarized 2D field, i.e., a field for which the spectral density in the x and y directions is the same, $\phi_{xx}(\mathbf{r},\omega) = \phi_{yy}(\mathbf{r},\omega)$, and for which no correlation exists between the two electric field components ($|\mu_{xy}(\mathbf{r},\omega)| = 0$), is passed through a polarizer. The 2D formalism gives the values $P_2(\mathbf{r},\omega) = 0$ and $P_2(\mathbf{r},\omega) = 1$ for the field before and after the polarizer, respectively. Let us now consider 3D fields in a similar way. Assume a fully unpolarized 3D field (lower part in Fig. 5), which is then polarized by two devices each cutting off one of the orthogonal field components. For a fully unpolarized 3D field, the spectral density in all three orthogonal directions is the same, $\phi_{xx}(\mathbf{r},\omega) = \phi_{yy}(\mathbf{r},\omega) = \phi_{zz}(\mathbf{r},\omega)$, and no correlations exist between any of the electric field components, i.e., $|\mu_{xy}(\mathbf{r},\omega)| = |\mu_{xz}(\mathbf{r},\omega)| = |\mu_{yz}(\mathbf{r},\omega)| = 0$. For this field, which cannot be described in terms of the 2D formalism, the 3D formalism gives the value of $P_3(\mathbf{r},\omega) = 0$ for the degree of polarization. When the

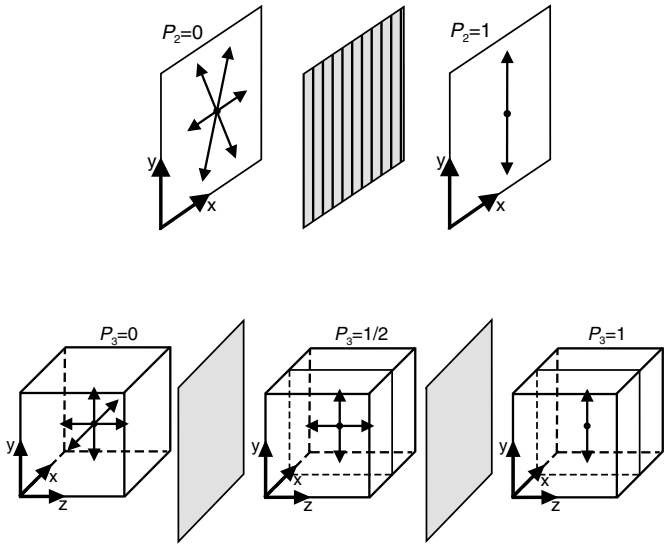

Figure 5: An illustration of the differences between the 2D and 3D coherence-matrix formalisms in treating the polarization state of an electromagnetic field.

x component of the field is cut off by the first device, the field becomes partially polarized. Indeed, now $\phi_{xx}(\mathbf{r},\omega) = 0$, $\phi_{yy}(\mathbf{r},\omega) = \phi_{zz}(\mathbf{r},\omega)$ with $|\mu_{yz}(\mathbf{r},\omega)| = 0$, and consequently $P_3(\mathbf{r},\omega) = 1/2$. The second device then cuts off the z component and the oscillations take place only in a single direction. Thus, the field becomes fully polarized with $P_3(\mathbf{r},\omega) = 1$.

We end this section by noting that in Ref. [60] it is argued that the value of the 3D degree of polarization for plane waves equals the value obtained by the 2D formalism. The above discussion points out that this conclusion is mistaken. In fact, the origin of the erroneous argument presented in Ref. [60] can be traced to an algebraic slip when Eq. (4.5.c) is reduced to Eq. (4.7) in Ref. [60].

4.4 Partial polarization in near-fields of thermal sources

The three-dimensional degree of polarization is a particularly useful tool for investigating the coherence properties of optical near fields. Recently, it has been theoretically demonstrated that the spectral and spatial-coherence properties of near fields emitted by thermal half-space sources contain interesting features. For example, due to the evanescent waves, the near-field spatial correlation length may be much shorter than the wavelength, or it may extend over several tens of wave-

lengths, when resonant surface waves, such as surface plasmons or phonons, are excited [66, 67]. Furthermore, the spectrum of the near field may differ from the source and far-field values, and it may even be quasimonochromatic when the surface waves are present [68]. Based on these results, it has been experimentally demonstrated that by diffracting the phonon field by a grating, highly coherent, directional emission from a thermal source can be obtained [69]. Motivated by these findings, we have assessed the influence of the evanescent waves and the resonant surface waves on the partial polarization of the near fields of thermally fluctuating half-space sources [Paper III].

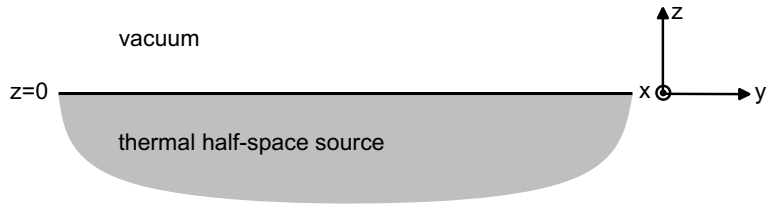

Figure 6: Illustration of the geometry used in analyzing the polarization of the near field of a thermal half-space source. The current distribution occupies the half space $z < 0$ and the half-space $z > 0$ is vacuum.

Coherence matrix of a thermal near field

We consider a thermal source occupying the half space $z < 0$ and separated from a vacuum by a sharp boundary at the plane $z = 0$ (see Fig. 6). The source consists of a homogeneous, isotropic and non-magnetic, lossy material, which is assumed to be in local thermodynamic equilibrium. The thermal current fluctuations are statistically stationary, homogeneous and isotropic, and they are explicitly described by the fluctuation-dissipation theorem [66, 68, 70]

$$\langle j_m^*(\mathbf{r}_1,\omega) j_n(\mathbf{r}_2,\omega')\rangle = \frac{\omega}{\pi}\epsilon_0\epsilon''(\omega)\Theta(\omega,T)\delta(\mathbf{r}_1-\mathbf{r}_2)\delta_{m,n}\delta(\omega-\omega'), \qquad (67)$$

where $\epsilon''(\omega)$ is the imaginary part of the dielectric constant of the material, and $\Theta(\omega, T)$ is the thermal energy of a quantum oscillator at temperature T. The electromagnetic field emitted by the source to the vacuum side can be calculated by employing the Green tensor technique for the surface geometry [51, 70]. In short, it consists of expressing the electromagnetic field produced by a point current as a superposition of vectorial plane waves (cf. Eq. (39)), then propagating the plane waves to the surface at $z = 0$, taking transmission into account in terms of the Fresnel coefficients, and then propagating the waves to the observation point. The calculation of the coherence-matrix elements in the geometry considered is outlined

in detail in Paper III. In order to supplement the presentation of Paper III, we give here the explicit forms of the coherence-matrix elements that were employed in the numerical calculations:

$$\Phi_{ij}(\mathbf{r},\omega) = 0, \qquad \text{when } i \neq j \tag{68}$$

$$\begin{aligned}\Phi_{xx}(\mathbf{r},\omega) &= \Phi_{yy}(\mathbf{r},\omega) \\ &= \zeta(\omega,T)\int_0^\infty \frac{|\mathbf{k}_\parallel|}{|\gamma_2|^2 \mathrm{Im}\gamma_2} \\ &\qquad \left[|t_s|^2 + \frac{|t_p|^2|\gamma_1|^2(|\gamma_2|^2+|\mathbf{k}_\parallel|^2)}{|\epsilon|k_0^4}\right] e^{(-2z\mathrm{Im}\gamma_1)}\,\mathrm{d}k_\parallel,\end{aligned} \tag{69}$$

$$\begin{aligned}\Phi_{zz}(\mathbf{r},\omega) &= 2\zeta(\omega,T)\int_0^\infty \frac{|\mathbf{k}_\parallel|}{|\gamma_2|^2 \mathrm{Im}\gamma_2} \\ &\qquad \left[\frac{|t_p|^2(|\gamma_2|^2+|\mathbf{k}_\parallel|^2)|\mathbf{k}_\parallel|^2}{|\epsilon|k_0^4}\right] e^{(-2z\mathrm{Im}\gamma_1)}\,\mathrm{d}k_\parallel.\end{aligned} \tag{70}$$

Here $\zeta(\omega,T) = \omega^3\mu_0^2\epsilon_0\epsilon''(\omega)\Theta(\omega,T)/32\pi^2$, and k_0 is the vacuum wave number. Furthermore, $\mathbf{k}_\parallel$ is the wave vector parallel to the surface, and $\gamma_1 = \sqrt{k_0^2 - |\mathbf{k}_\parallel|^2}$ and $\gamma_2 = \sqrt{\epsilon k_0^2 - |\mathbf{k}_\parallel|^2}$ with $\mathrm{Im}\,\gamma_i > 0$, ($i = 1, 2$), are the components of wave vectors perpendicular to the surface in vacuum and in the source region, respectively. Moreover, $t_s = 2\gamma_2/(\gamma_1+\gamma_2)$ and $t_p = 2\gamma_2\sqrt{\epsilon}/(\epsilon\gamma_1+\gamma_2)$ are the ($\mathbf{k}_\parallel$-dependent) Fresnel transmission coefficients for s- and p-polarized waves.

Surface polaritons

Resonant surface waves, e.g., surface-plasmon and surface-phonon polaritons are mechanical collective excitations involving charges [71, 72]. Surface-plasmon polaritons are oscillations of the density of the free electrons in a metal, whereas the surface-phonon polaritons are lattice vibrations, i.e., phonons in a polar material. Since the polaritons are charge-density waves they generate an electromagnetic field. The field decays exponentially in the direction perpendicular to the surface, but propagates parallel to it. The propagation length may be several tens of wavelengths, depending on the dissipation in the medium. Thus, the surface waves can mediate long-distance spatial correlations, and this is the physical origin of the spatial correlation phenomena reported in Ref. [66, 67]. The surface waves can be excited at the interface between the material and the vacuum provided that the permittivity of the material satisfies the relation $\mathrm{Re}\{\epsilon(\omega)\} < -1$ [71]. Only p-polarized light can excite surface waves, a fact which is mathematically related to the presence of a pole in the corresponding Fresnel coefficient. The location of the pole determines the dispersion relation for the surface polaritons at the material-vacuum

interface [71],

$$k_{SW}^2(\omega) = k_0^2 \frac{\epsilon(\omega)}{\epsilon(\omega)+1}. \tag{71}$$

Moreover, the polariton waves are known to be highly polarized in the plane spanned by their direction of propagation and the surface normal.

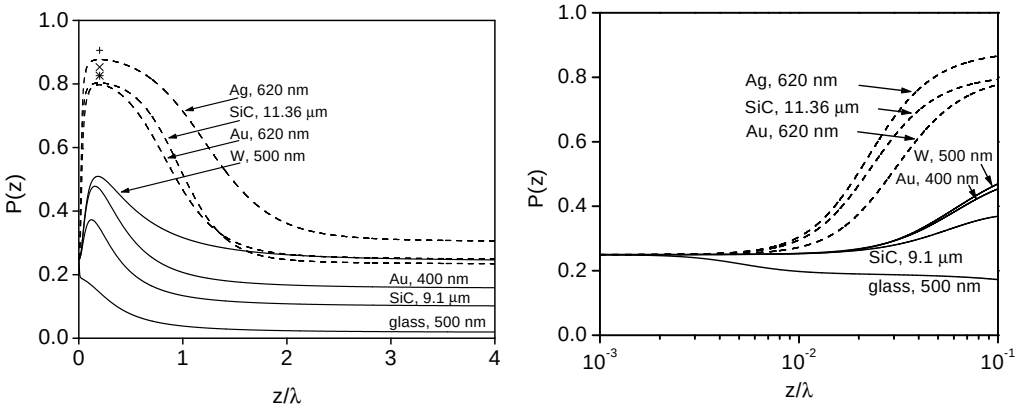

Figure 7: Behavior of the degree of polarization as a function of distance z from the surface for some materials at $T = 300$ K, (a) $0 < z < 4\lambda$, (b) $10^{-3}\lambda < z < 10^{-1}\lambda$.

Degree of polarization

We now apply the formalism for the 3D degree of polarization to analyze the near field in the geometry of Fig. 6 for some particular materials. Figures 7(a) and 7(b) illustrate the degree of polarization as a function of the distance from the surface at wavelength $\lambda = 620$ nm for gold and silver, at $\lambda = 500$ nm for lossy glass and tungsten, at $\lambda = 400$ nm for gold, and at the wavelengths $\lambda = 11.36$ μm and $\lambda = 9.1$ μm for silicon carbide (SiC). The values of the dielectric constants of the materials considered are listed in Paper III.

We first note that glass does not support surface plasmons or phonons and, consequently, the degree of polarization in the near field for glass decays monotonically within a wavelength and settles down to a constant value. This indicates that the evanescent waves, which are strong only within $z < \lambda$, have a clear effect on the near-field polarization. At the wavelength $\lambda = 620$ nm both gold and silver have a plasmon resonance, and consequently, the near field is strongly polarized as is seen in Fig. 7(a). The near-field degrees of polarization for both gold and silver

have values as high as 0.80 and 0.88, respectively, at the distance of $z \approx 0.2\lambda$ from the surface. On the other hand, for gold at wavelength $\lambda = 400$ nm, for which $\mathrm{Re}\{\epsilon(\omega)\} = -1.1$, the plasmon effect is greatly reduced. Similarly, in the case of tungsten at $\lambda = 500$ nm, for which $\mathrm{Re}\{\epsilon(\omega)\} > -1$ and no surface plasmons exist, the peak in the near field is substantially smaller. Furthermore, as evidenced by the curve for SiC at wavelength the $\lambda = 11.36$ μm, the surface phonons also strongly polarize the near field. When the wavelength of light is off from the phonon resonance ($\lambda = 9.1$ μm), the degree of polarization reduces significantly.

As regards the abrupt reduction of the degree of polarization immediately above the surface in the very near field, we point out that very close to the surface the so-called quasi-static field which depends on the distance as $1/(k_0 z)^3$, starts to dominate over the polariton or any other effects [67]. It can be analytically verified that at the limit $z \to 0$ the ratios of the coherence-matrix elements of Eqs. (68)–(70) are as $\Phi_{xx}(\mathbf{r}, \omega) = \Phi_{yy}(\mathbf{r}, \omega) = \Phi_{zz}(\mathbf{r}, \omega)/2$, which directly gives $P_3 = 1/4$, regardless of the material. This behavior is illustrated in Fig. 7(b). Furthermore, when the surface polaritons strongly contribute to the field, one can show that the diagonal elements of the coherence matrix are related as $\Phi_{xx}(\mathbf{r}, \omega) = \Phi_{yy}(\mathbf{r}, \omega) = \Phi_{zz}(\mathbf{r}, \omega)/2|\epsilon(\omega)|$. In Fig. 7(a), the approximative values for the degrees of polarization in the case of strong polariton effects, are plotted as symbols $+$ and $\times$ for silver and gold, respectively, and as $*$ for SiC. As regards the far-zone values of the degrees of polarization for the different materials (see Fig. 7(a)), we note that if the whole space would be filled with a thermal material, the radiation in it would be isotropic. However, the boundary surface breaks the isotropy and the way it is broken depends on the materials that constitute the boundary. Thus the far-zone degree of polarization must be material dependent. A closely related topic is encountered in the next section, where we examine the field inside statistically homogeneous and isotropic source regions.

4.5 Partial polarization in homogeneous free fields

We next apply the formalism of the 3D degree of polarization to study the polarization of free electromagnetic fields [Paper IV]. The field is assumed to consists of a superposition of unpolarized (in the 2D sense) and angularly uncorrelated plane waves, which are isotropically distributed within a cone of angles. The medium is taken to be homogeneous, isotropic and non-dissipative. The polarization behavior is analyzed as a function of the cone angle, and the important special case of isotropic distribution within the full angle is discussed in some detail.

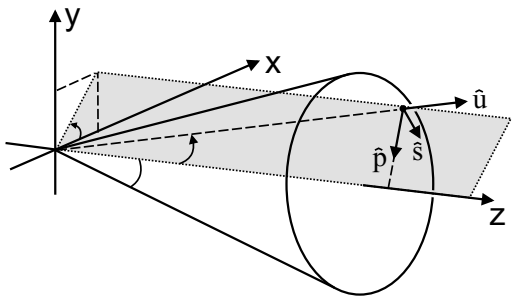

Figure 8: Illustration of notations for treating partial polarization in a homogeneous free field. The propagation direction of a plane wave, represented by the azimuth (φ) and polar (θ) angles in a spherical polar coordinate system, and denoted by the unit vector $\hat{u}$, is restricted to a cone having the cone angle α. The unit vectors $\hat{s}$ and $\hat{p}$, correspond to the s and p polarizations, respectively.

Electric cross-spectral density tensor

The geometry and notations are illustrated in Fig. 8. The electric cross-spectral density tensor for the field that we consider can be shown to have the form [Paper IV]

$$\overleftrightarrow{W}(\mathbf{r}_1, \mathbf{r}_2, \omega) = a_0(\omega) \int_\Omega (\overleftrightarrow{U} - \hat{u}\hat{u}) \exp(-ik\hat{u} \cdot \mathbf{r}) \mathrm{d}\Omega, \tag{72}$$

where $\hat{u}$ is a unit vector specifying the propagation direction of a plane wave, and the integration is performed over the solid angle Ω that covers all propagation directions within the cone. Furthermore, since the plane waves are assumed to be angularly uncorrelated, the cross-spectral density tensor depends only on the separation of the two points of observation, $\mathbf{r} = \mathbf{r}_1 - \mathbf{r}_2$, thus indicating that the field is statistically homogeneous [74]. The assumption that the plane waves are unpolarized is included in Eq. (72) through the fact that their s- and p-polarized components do not correlate, and that the spectral density, $a_0(\omega)$, is the same for these two polarization directions. Furthermore, $a_0(\omega)$ is independent of the wave's propagation direction within the cone, since the wave distribution is taken to be isotropic.

At this stage, we make an important remark to which we shall return in the next section. Namely, when the isotropic distribution of the plane waves covers the full solid angle, i.e. $\Omega = 4\pi$, the cross-spectral density tensor of Eq. (72) takes on the form [Paper IV]

$$\overleftrightarrow{W}(\mathbf{r}, \omega) = \frac{4\pi a_0(\omega)}{k} \mathrm{Im}\left[\overleftrightarrow{G}(\mathbf{r}, \omega)\right]. \tag{73}$$

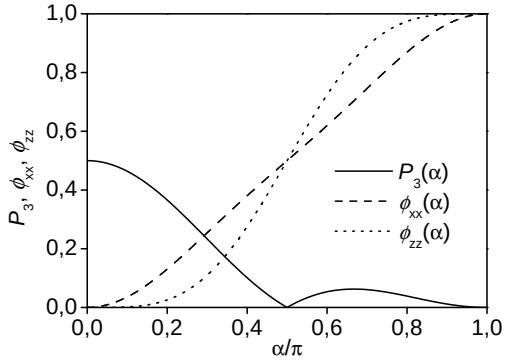

Figure 9: Behavior of the 3D degree of polarization $P_3(\alpha)$ (solid line), and the normalized coherence-matrix elements $\phi_{xx}(\alpha)$ (dashed line) and $\phi_{zz}(\alpha)$ (dotted line), as a function of the cone angle α.

Thus, the cross-spectral density tensor is proportional to the imaginary part of the Green tensor of the system. By choosing the spectral coefficient $4a_0(\omega)$ to match with Planck's law, Eq. (73) becomes identical with the cross-spectral tensor of black-body radiation [75, 76]. Therefore, within the simple physical picture of (in the 2D sense) unpolarized, angularly uncorrelated, and isotropically distributed plane waves, the known results of black-body fields are recovered, without assuming thermal equilibrium. We note that in Ref. [77] an analogous results was obtained by considering a scalar field consisting of angularly uncorrelated and isotropically distributed scalar plane waves. For this field the degree of coherence is proportional to the imaginary part of the associated Green function, being explicitly given by a sinc function.

Degree of polarization

The 3×3 coherence matrix as a function of the cone angle α can be calculated from Eq. (72) by first taking the limit $\mathbf{r} \to \mathbf{0}$ and then performing the angular integrations. The resulting expression for the coherence matrix, $\Phi_3(\alpha, \omega)$, is diagonal, as expected for a field consisting of unpolarized and uncorrelated plane waves, with the diagonal elements having the form

$$\Phi_{xx}(\alpha, \omega) = \Phi_{yy}(\alpha, \omega) = \frac{\pi a_0(\omega)}{12} \left[16 - 15\cos(\alpha) - \cos(3\alpha)\right], \tag{74}$$

and

$$\Phi_{zz}(\alpha, \omega) = \frac{\pi a_0(\omega)}{6} \left[8 - 9\cos(\alpha) + \cos(3\alpha)\right]. \tag{75}$$

On substituting Eqs. (74) and (75) into Eq. (62), we find that

$$P_3(\alpha) = \frac{1}{4}(1 + \cos\alpha)|\cos\alpha|. \tag{76}$$

The behavior of the degree of polarization and the normalized coherence-matrix elements as a function of the cone angle α are shown in Fig. 9. For $\alpha = 0$, i.e., when the electromagnetic field consists only of a single unpolarized plane wave, Eq. (62) for the 3D degree of polarization gives $P_3 = 1/2$. The conventional 2D formalism would, of course, give a value of $P_2 = 0$ as was discussed in Sec. 4.2. When the cone angle α is increased from zero, the intensities of the three field components grow monotonically as more plane waves are included. The intensities of the x and y components are, at first, greater than that of the z component, which, however, with increasing α grows more rapidly. Since the three orthogonal field components are mutually uncorrelated for all values of α, the degree of polarization decreases with an increasing value of α until the electromagnetic field consists of plane waves propagating in all directions in the half-space $z > 0$, i.e., when $\alpha = \pi/2$. In this situation, the intensities of the x, y and z components are the same and the field is fully unpolarized. When the cone angle is increased further, the degree of polarization increases again, since the energy of the z component exceeds the energy of the x and y components. Finally, when $\alpha = \pi$, corresponding to the case of unpolarized plane waves propagating into the full 4π solid angle, the intensities of the different components become equal again, and consequently $P_3 = 0$. As noted in connection with Eq. (73), the case of full solid angle corresponds to the black-body field. Thus, the value $P_3 = 0$ is consistent with the common notion that the black-body field is fully unpolarized.

5 Electromagnetic Field Correlations within Homogeneous and Isotropic Sources

Recent investigations show that the spatial correlations of scalar fields produced by stationary, statistically homogeneous and isotropic sources in low-loss media have a remarkable universal character [78, 79]. The spectral degree of coherence of any such field in two or three dimensional space is proportional to the imaginary part of the Green function of the system, indicating that the correlations are entirely determined by the propagation properties in the medium, not by the source characteristics. For such a field, the degree of coherence at two points $\mathbf{r}_1$ and $\mathbf{r}_2$ is in three dimensions explicitly given by the sinc function $\sin(k|\mathbf{r}_1-\mathbf{r}_2|)/(k|\mathbf{r}_1-\mathbf{r}_2|)$ [78,79], which we later on make a reference to as the sinc law. In two dimensions the dependence follows the zero-order Bessel function $J_0(k|\mathbf{r}_1-\mathbf{r}_2|)$ [79]. The sinc law has previously been found also for the low-frequency part of statistically homogeneous planar Lambertian sources [75], and for the field within a completely incoherent primary spherical source [80].

In Paper V, we investigate the spatial correlations in the electromagnetic fields produced by statistically homogeneous and isotropic current sources. We find that for such fields, provided that the medium has vanishingly small absorption, the electric cross-spectral density tensor is proportional to the imaginary part of the Green tensor of the system. Consequently, the normalized trace of the Green tensor, or the field's degree of coherence obeys the sinc law. This result restores the known results of black-body fields [70, 76], but it is true for a wider class of sources, not required to be in thermal equilibrium. Our results generalize the scalar results of Refs. [78, 79] to homogeneous and isotropic electromagnetic fields.

In the following, we outline the main steps of the calculation for expressing the cross-spectral density tensor of the field in terms of the corresponding source tensor. This result is then applied to statistically homogeneous and isotropic source distributions and the degree of coherence and the degree of polarization of the field produced by such a source is analyzed. We also provide a physical explanation to the universal behavior of the correlations by making use of the electromagnetic plane wave model discussed in Sec. 4.5.

5.1 Spatial correlations in the field produced by a statistically homogeneous source

In a homogeneous, isotropic and linear medium, the monochromatic field and current realizations (at the frequency ω) obey the inhomogeneous vector wave equa-

tion,

$$\nabla \times \nabla \times \mathbf{E}(\mathbf{r}', \omega) - \kappa^2 \mathbf{E}(\mathbf{r}', \omega) = i\omega\mu \mathbf{j}(\mathbf{r}', \omega). \tag{77}$$

Here $\kappa = k_0 n$, with k_0 being the free-space wave number, and n is the complex refractive index of the medium, which is expressed as $n = \sqrt{\epsilon_r \mu_r}$ in terms of the relative permittivity, ϵ_r, and permeability, μ_r. Making use of Eq. (77), it is straightforward to prove that the spatial Fourier transforms of the field and of the current density, defined by

$$\tilde{\mathbf{E}}(\mathbf{k}, \omega) = \int d^3 r' \, \mathbf{E}(\mathbf{r}', \omega) e^{-i\mathbf{k}\cdot\mathbf{r}'}, \tag{78}$$

$$\tilde{\mathbf{j}}(\mathbf{k}, \omega) = \int d^3 R' \, \mathbf{j}(\mathbf{R}', \omega) e^{-i\mathbf{k}\cdot\mathbf{R}'}, \tag{79}$$

are related as

$$\tilde{\mathbf{E}}(\mathbf{k}, \omega) = -\frac{i\eta_0}{k_0 \epsilon_r (k^2 - \kappa^2)} \left(\mathbf{k}\mathbf{k} - \kappa^2 \overleftrightarrow{U} \right) \cdot \tilde{\mathbf{j}}(\mathbf{k}, \omega), \tag{80}$$

where $\eta_0 = \sqrt{\mu_0/\epsilon_0}$ is the vacuum impedance. Statistical homogeneity implies that the different Fourier components of the (infinite) source are delta correlated, and we find the following expression for the electric cross-spectral density tensor of the field fluctuating in the low-loss medium [Paper V]

$$\overleftrightarrow{W}_{ee}(\mathbf{r}, \omega) = \frac{\eta_0^2 \mu_r}{\epsilon_r''} \left(\overleftrightarrow{U} + \frac{1}{\kappa^2} \nabla_{\mathbf{r}} \nabla_{\mathbf{r}} \right) \cdot \int d^3 R \;\; \overleftrightarrow{W}_{jj}(\mathbf{R}, \omega) \cdot \mathrm{Im} \left[\overleftrightarrow{G}(\mathbf{r} - \mathbf{R}, \omega) \right]. \tag{81}$$

In this equation the parameter ϵ_r'' denotes the imaginary part of the relative permittivity, and $\overleftrightarrow{G}(\mathbf{r} - \mathbf{R}, \omega)$ is the associated Green tensor, given in Eq. (34) for $\kappa = k_0$. The tensor $\overleftrightarrow{W}_{jj}(\mathbf{R}, \omega)$ is the cross-spectral density tensor of the source, which, due to the homogeneity depends on the difference $\mathbf{R} = \mathbf{R}_1 - \mathbf{R}_2$ between two source points $\mathbf{R}_1$ and $\mathbf{R}_2$. Furthermore, $\overleftrightarrow{W}_{ee}(\mathbf{r}, \omega)$ depends only on the separation $\mathbf{r} = \mathbf{r}_1 - \mathbf{r}_2$, indicating that the field generated by a statistically homogeneous source is also statistically homogeneous.

5.2 Spatial correlations in the field produced by a statistically homogeneous and isotropic source

The general expression for the cross-spectral density tensor of a source, which is not only statistically homogeneous, but also isotropic, is of the form [81, 82]

$$\overleftrightarrow{W}_{jj}(\mathbf{R}, \omega) = A(R, \omega) \overleftrightarrow{U} + B(R, \omega) \hat{\mathbf{R}} \hat{\mathbf{R}}, \tag{82}$$

where $A(R,\omega)$ and $B(R,\omega)$ are scalar functions, and $\hat{\mathbf{R}} = \mathbf{R}/R$ with $R = |\mathbf{R}|$. In fact, the functions $A(R,\omega)$ and $B(R,\omega)$ are not entirely independent, but are connected by a continuity equation. Equation (82) is symmetric and its form is invariant under rotation of the coordinate system.

By inserting Eq. (82) into Eq. (81) one finds that [Paper V]

$$\overleftrightarrow{W}_{ee}(\mathbf{r},\omega) = \frac{4\pi\eta_0^2\mu_r}{\epsilon_r''}\left[C_A(\omega) + C_B(\omega)\right] \mathrm{Im}\left[\overleftrightarrow{G}(\mathbf{r},\omega)\right], \tag{83}$$

where the spectral coefficients are

$$C_A(\omega) = \int_0^\infty dR R^2 A(R,\omega) j_0(\kappa R), \tag{84}$$

and

$$C_B(\omega) = \int_0^\infty dR R^2 B(R,\omega) \frac{j_1(\kappa R)}{\kappa R}, \tag{85}$$

with $j_l(\kappa\omega)$, $l = 0, 1$, being spherical Bessel functions of the first kind and of order l.

Degree of coherence

Equation (83) shows that the spatial correlation properties of an electromagnetic field generated by any statistically homogeneous and isotropic source distribution within a low-loss medium are determined by the imaginary part of the Green tensor of the system. In particular, the normalized trace of the electric cross-spectral density tensor, often regarded as the electromagnetic field's degree of spatial coherence [75, 83–85], assumes the form

$$\mu_{ee}(\mathbf{r},\omega) = \frac{\mathrm{tr}\left[\overleftrightarrow{W}_{ee}(\mathbf{r},\omega)\right]}{\mathrm{tr}\left[\overleftrightarrow{W}_{ee}(\mathbf{0},\omega)\right]} = \frac{\sin\kappa r}{\kappa r} = \frac{4\pi}{\kappa}\mathrm{Im}\left[G(\mathbf{r},\omega)\right], \tag{86}$$

where $r = |\mathbf{r}|$, and $G(\mathbf{r},\omega)$ is the spherical wave given by Eq. (35) with k_0 replaced by κ. Equation (86) shows that the degree of coherence of the field does not depend on the source characteristics, but on the propagation properties of the field in the medium. This result generalizes the scalar results of Refs. [78, 79] to the case of homogeneous and isotropic electromagnetic fields.

We noted in Sec. 4.5 that for a field consisting of a superposition of unpolarized, angularly uncorrelated plane waves which are isotropically distributed within the full solid angle, the electric cross-spectral density tensor is proportional to the imaginary

part of the Green tensor (see Eq. (73)). Thus, the correlations in such a field also obey the sinc law of Eq. (86). Furthermore, the fluctuation-dissipation theorem for the source correlations, Eq. (67), is of the form of Eq. (82). Therefore, for the field generated by a source for which the correlations obey the fluctuation-dissipation theorem and which occupies the entire space, the correlations are characterized by the sinc law. For the thermal half-space source considered in Sec. 4.4, the isotropy is, however, broken due to the boundary surface, and consequently the sinc law is not found.

Degree of polarization

To calculate the 3D degree of polarization for a field with spatial correlations proportional to the imaginary part of the Green tensor, we take the limit $\mathbf{r} \to \mathbf{0}$ in Eq. (83) and obtain for the coherence tensor

$$\Phi_3(\omega) = \frac{2\kappa\eta_0^2\mu_r}{3\epsilon_r''}\left[C_A(\omega) + C_B(\omega)\right] \overleftrightarrow{U} \,. \tag{87}$$

This, when inserted into Eq. (62), yields $P_3(\omega) = 0$. Thus, the field within any statistically homogeneous and isotropic current distribution is fully unpolarized. To a good approximation, this result holds also for the field at points well inside a large, but finite, source region. On the other hand, the far field produced by a large statistically homogeneous and isotropic source domain is, in the 2D sense, fully unpolarized in every direction [Paper V]. This corresponds to the value $P_3(\mathbf{r}, \omega) = 1/2$ in the 3D formalism. Therefore, the value of the 3D degree of polarization increases from $P_3(\mathbf{r}, \omega) = 0$ to $P_3(\mathbf{r}, \omega) = 1/2$ when the observation point moves from inside the source to the far zone.

5.3 Comparison with a plane-wave model

Physical insight into the universal behavior of correlations in electromagnetic fields can be obtained by considering the field inside an infinite, statistically homogeneous and isotropic source domain as a superposition of plane waves. The arguments are parallel to those presented in Ref. [77] for the scalar case, but go somewhat beyond those because of the vectorial nature of the electromagnetic field.

Since the medium has a small but non-zero absorption, the field correlations extend effectively over a finite region in the neighborhood of a given source point. Therefore, we may think of the whole infinite source as being divided into finite, uniformly distributed, and mutually uncorrelated domains whose dimensions depend on the correlation length. We refer to these domains as source correlation regions. Each source correlation region produces an electromagnetic field, which

at large distances behaves approximately as a plane wave. Thus, in any observation region, the contributions from the (very) distant parts of the source can be viewed as consisting of a superposition of isotropically distributed and angularly uncorrelated plane waves. For source regions containing statistically homogeneous and isotropic current distributions, these plane waves are also fully unpolarized in the 2D sense [Paper V]. In Sec. 4.5 we found that for a field consisting of unpolarized, angularly uncorrelated and isotropically distributed plane waves, the spatial correlations are determined by the imaginary part of the Green tensor (Eq. (73)). Hence, the plane-wave model and the calculations presented in this section show that the field correlations in any observation region are determined by the distant contributions. Although the local currents at every point also generate a near field, with the associated correlation tensor having both real and imaginary parts [Paper I], this contribution from a statistically homogeneous and isotropic current in an infinite low-loss or non-absorbing medium is negligible as compared to the propagating far-zone contributions. Thus, despite of the local current sources, the field at any point behaves effectively as a free electromagnetic field.

When the losses are significant, the correlations do not show any universal behavior as noted in Ref. [79]. This can be physically explained by using the plane-wave model discussed above. In the presence of losses, the contribution to the field from the distant source correlation regions weakens in relation to that from the nearby regions. Consequently, the plane-wave model no longer describes the physical situation, and no universality is found.

6 Summary and Conclusions

In this thesis, certain fundamental issues related to optical near-fields are studied. The nature of the evanescent and propagating field components generated by a point-dipole source are discussed. The concept of three-dimensional degree of polarization is introduced to cover electromagnetic fields having arbitrary planar or non-planar wave structures. Its physical interpretation is presented, and the differences compared with the conventional two-dimensional theory are brought out. The theory is applied to investigate the effects of evanescent waves and resonant surface waves on the polarization state of the near fields generated by some thermal half-space sources. The novel theory for the three-dimensional degree of polarization is expected to be particularly useful for the polarization studies of random electromagnetic fields having three orthogonal field components, such as optical near fields.

The thesis also includes a study of the partial polarization and spatial correlation properties of homogeneous free electromagnetic fields. The fields are modelled as an isotropic distribution of angularly uncorrelated and in the 2D-sense unpolarized plane waves propagating within a solid angle. In the case of the full solid angle, the spatial correlations are found to be determined by the imaginary part of the associated Green tensor, and the field is fully unpolarized in the three-dimensional sense. These results are the same as for black-body fields, although no thermal equilibrium was assumed. The same behavior is discovered for any electromagnetic field generated by a statistically homogeneous and isotropic current distribution fluctuating within a medium having vanishingly small absorption. For the fields whose electric cross-spectral density tensor is proportional to the imaginary part of the Green tensor, the degree of coherence is of a universal form given by the sinc law.

In the thesis, we could only treat a restricted number of issues relevant to obtaining a thorough understanding of the coherence properties of the optical near fields. In fact, several interesting research subjects emerged during the work, such as the question on how many of the generalized Stokes parameters needed to describe the three-dimensional degree of polarization really are independent and what are their explicit connections. How the three-dimensional degree of polarization, or the near-field Stokes parameters, could be measured is an issue of particular importance in near-field optics. Furthermore, it is known that the 2D degree of polarization is related to the entropy of the field. What is the corresponding relation between the entropy and the 3D degree of polarization is an open question. In addition, an investigation on the effects of dissipation on the spatial correlation of fields within statistically homogeneous and isotropic source regions would be of genuine interest.

References

[1] F. de Fornel, *Evanescent Waves* (Springer, Berlin, 2001).

[2] P. Meystre, *Atom Optics* (Springer, New York, 2001).

[3] M. Ohtsu and H. Hori, *Near-Field Nano-Optics* (Kluwer, New York, 1999).

[4] J. P. Fillard, *Near-Field Optics and Nanoscopy* (World Scientific, Singapore, 1996).

[5] M. A. Paesler and P. J. Moyer, *Near-Field Optics: Theory, Instrumentation and Applications* (Wiley, New York, 1996).

[6] J.-J. Greffet and R. Carminati, "Image formation in near-field optics", Prog. Surf. Sci. **56**, 133–237 (1997).

[7] C. Girard, C. Joachim, and S. Gauthier, "The physics of the near field", Rep. Prog. Phys. **63**, 893–938 (2000).

[8] P. F. Barbara, D. M. Adams, and D. B. O'Connor, "Characterization of organic thin film materials with near-field scanning optical microscopy (NSNOM)", Annu. Rev. Mater. Sci. **29**, 433–469 (1999).

[9] R. C. Dunn, "Near-field scanning optical microscopy", Chem. Rev. **99**, 2891–2927 (1999).

[10] B. Hecht, B. Sick, U. P. Wild, V. Deckert, R. Zenobi, O. J. F. Martin, and D. W. Pohl, "Scanning near-field oprical microscopy with aperture probes: fundamentals and applications", J. Chem. Phys. **112**, 7761–7774 (2000).

[11] C. Girard and A. Dereux, "Near-field optics theories", Rep. Prog. Phys. **59**, 657–699 (1996).

[12] D. Van Labeke and D. Barchiesi, "Scanning-tunneling optical microscopy: a theoretical macroscopic approach", J. Opt. Soc. Am. A **9**, 732–739 (1992).

[13] E. Vasilyeva and A. Taflove, "Three-dimensional modeling of amplitude-object imaging in scanning near-field optical microscopy", Opt. Lett. **23**, 1155–1157 (1998).

[14] C. M. Kelso, P. D. Flammer, J. A. DeSanto, and R. T. Collins, "Integral equations applied to wave propagation in two dimensions: modeling the tip of a near-field scanning optical microscope", J. Opt. Soc. Am. A **18**, 1993–2001 (2001).

[15] L. Mandel and E. Wolf, *Optical Coherence and Quantum Optics* (Cambridge University Press, Cambridge, UK, 1995).

[16] M. Born and E. Wolf, *Principles of Optics*, 7th Ed. (Cambridge University Press, Cambridge, UK, 1999).

[17] J. Peřina, *Coherence of Light* (Reidel, Dordrecht, 1985).

[18] J. W. Goodman, *Statistical Optics* (Wiley, New York, 1985).

[19] C. Brosseau, *Fundamentals of Polarized Light: A Statistical Optics Approach* (Wiley, New York, 1998).

[20] T. B. Hansen and A. D. Yaghjian, *Plane-Wave Theory of Time-Domain Fields* (IEEE Press, New York, 1999).

[21] P. Roman and E. Wolf, "Correlation theory of stationary electromagnetic fields. Part I: the basic field equations", Nuovo Cimento **17**, 462–476 (1960).

[22] E. Wolf, "New theory of partial coherence in the space-frequency domain. Part I: spectra and cross spectra of steady-state sources", J. Opt. Soc. Am. **72**, 343–351 (1982).

[23] E. Wolf and J. T. Foley, "Do evanescent waves contribute to the far field?", Opt. Lett. **23**, 16–18 (1998).

[24] A. V. Shchegrov and P. S. Carney, "Far-field contribution of evanescent modes to the electromagnetic Green tensor", J. Opt. Soc. Am. A **16**, 2583–2584 (1999).

[25] O. Keller, "Attached and radiated electromagnetic fields of an electric point dipole", J. Opt. Soc. Am. B **16**, 835–847 (1999).

[26] A. Rahmani and G. W. Bryant, "Contribution of evanescent waves to the far field: the atomic point of view", Opt. Lett. **25**, 433–435 (2000).

[27] P. S. Carney, D. G. Fisher, J. T. Foley, A. T. Friberg, A. V. Shchegrov, T. D. Visser, and E. Wolf, "Evanescent waves do contribute to the far field: comment", J. Mod. Opt. **47**, 757–758 (2000).

[28] A. Lakhtakia and W. S. Weiglhofer, "Evanescent plane waves and the far field: resolution of a controversy", J. Mod. Opt. **47**, 759–763 (2000).

[29] C. J. R. Sheppard and F. Aguilar, "Evanescent fields do contribute to the far field: comment", J. Mod. Opt. **48**, 177–180 (2001).

[30] T. Setälä, M. Kaivola, and A. T. Friberg, "Evanescent and propagating electromagnetic fields in scattering from point-dipole structures", J. Opt. Soc. Am. A **18**, 678–688 (2001).

[31] M. V. Berry, "Asymptotics of evanescence", J. Mod. Opt. **48**, 1535–1541 (2001).

[32] H. F. Arnoldus and J. T. Foley, "Traveling and evanescent parts of the electromagnetic Green's tensor", J. Opt. Soc. Am. A **19**, 1701–1711 (2002).

[33] H. F. Arnoldus and J. T. Foley, "Uniform asymptotic approximation of the evanescent part of the Green's tensor", Opt. Comm. **207**, 7–15 (2002).

[34] T. Setälä, M. Kaivola, and A. T. Friberg, "Evanescent and propagating electromagnetic fields in scattering from point-dipole structures: reply to comment", J. Opt. Soc. Am. A **19**, 1449–1451 (2002).

[35] G. C. Sherman, J. J. Stamnes, A. J. Devaney, É. Lalor, "Contribution of the inhomogeneous waves in angular-spectrum representations", Opt. Comm. **8**, 271–274 (1973).

[36] G. C. Sherman, J. J. Stamnes and É. Lalor, "Asymptotic approximations to angular-spectrum representations", J. Math. Phys. **17**, 760–776 (1976).

[37] D. C. Bertilone, "The contributions of homogeneous and evanescent plane waves to the scalar optical field: exact diffraction formulae", J. Mod. Opt. **38**, 865–875 (1991).

[38] M. Xiao, "Cutting off the diffraction: a numerical solution in scanning near-field optical microscopy", Appl. Phys. Lett. **69**, 3125–3127 (1996).

[39] M. Xiao, "A study of resolution limit in optical microscopy: near and far field", Opt. Comm. **132**, 403–409 (1996).

[40] M. Xiao, "Evanescent field coupling of dipole to a surface: configurational resonance at long distances", Chem. Phys. Lett. **258**, 363–368 (1996).

[41] M. Xiao, "Polarization effects in reflection scanning near field optical microscopy", Opt. Comm. **136**, 213–218 (1997).

[42] M. Xiao, "Two-point optical resolution with homogeneous, evanescent and self field: resolution criterion in near field imaging", J. Mod. Opt. **44**, 1609-1615 (1997).

[43] M. Xiao, "On near-field scanning optical microscopy: homogeneous and evanescent radiation", J. Mod. Opt. **44**, 327–344 (1997).

[44] M. Xiao, A. Zayats, and J. Siqueiros, "Scattering of surface-plasmon polaritons by dipoles near a surface: Optical near-field localization", Phys. Rev. B **55**, 1824–1837 (1997).

[45] M. Xiao and X. Chen, "Optical dipole radiation inside nanometric planar two-surface systems", Opt. Comm. **158**, 11–17 (1998).

[46] M. Xiao, "Evanescent waves do contribute to the far field", J. Mod. Opt. **46**, 729–733 (1999).

[47] M. Xiao, "Reply: On the evanescent field of dipole", J. Mod. Opt. **47**, 765–768 (2000).

[48] M. Xiao, "Optical fiber tip in front of a phase conjugator: focused light spot with inclusion of evanescent field contribution", Appl. Phys. A **64**, 91–99 (1997).

[49] M. Xiao, "Evanescent and propagating electromagnetic fields in scattering from point-dipole structures: comment", J. Opt. Soc. Am. A **19**, 1447–1448 (2002).

[50] C.-T. Tai, *Dyadic Green's Functions in Electromagnetic Theory*, (Intext, Scranton, PA, 1971).

[51] J. E. Sipe, "A new Green-function formalism for surface optics", J. Opt. Soc. Am. B **4**, 481–489 (1987).

[52] E. Wolf, "Coherence properties of partially polarized electromagnetic radiation", Nuovo Cimento **13**, 1165–1181 (1959).

[53] F. Gori, M. Santarsiero, S. Vicalvi, R. Borghi, and G. Guattari, "Beam coherence-polarization matrix", Pure Appl. Opt. **7**, 941–951 (1998).

[54] D. F. V. James, "Polarization of light radiated by black-body sources", Opt. Comm. **109**, 209–214 (1994).

[55] G. Gbur and D. F. V. James, "Unpolarized sources that generate highly polarized fields outside the source", J. Mod. Opt. **47**, 1171–1177 (2000).

[56] J. C. Samson, "Descriptions of the polarization states of vector processes: applications to ULF magnetic fields", Geophys. J. R. Astr. Soc. **34**, 403–419 (1973).

[57] J. C. Samson and J. V. Olson, "Some comments on the descriptions of the polarization states of waves", Geophys. J. R. Astr. Soc. **61**, 115–129 (1980).

[58] J. C. Samson, ”Comments on polarization and coherence”, J. Geophys. **48**, 195–198 (1980).

[59] R. Barakat, ”Degree of polarization and the principal idempotents of the coherency matrix”, Opt. Commun. **23**, 147–150 (1977).

[60] R. Barakat, ”*n*-Fold polarization measures and associated thermodynamic entropy of *N* partially coherent pencils of radiation”, Opt. Acta **30**, 1171–1182 (1983).

[61] C. Brosseau, ”Entropy of a classical stochastic wavefield: effect of polarization”, Optik **104**, 21–26 (1996).

[62] C. Brosseau, ”Entropy and polarization of a stochastic radiation field”, Prog. Quant. Electr. **21**, 421–461 (1997).

[63] T. Carozzi, R. Karlsson, and J. Bergman, ”Parameters characterizing electromagnetic wave polarization”, Phys. Rev. E **61**, 2024–2028 (2000).

[64] P. Roman, ”Generalized Stokes parameters for waves with arbitrary form”, Nuovo Cimento **13**, 974–982 (1959).

[65] M. Gell-Mann and Y. Ne’eman, *The Eightfold Way* (Benjamin, New York, 1964).

[66] R. Carminati and J.-J. Greffet, ”Near-field effects in spatial coherence of thermal sources”, Phys. Rev. Lett. **82**, 1660–1663 (1999).

[67] C. Henkel, K. Joulain, R. Carminati, and J.-J. Greffet, ”Spatial coherence of thermal near fields”, Opt. Comm. **186**, 57–67 (2000).

[68] A. V. Shchegrov, K. Joulain, R. Carminati, and J.-J. Greffet, ”Near-field spectral effects due to electromagnetic surface excitations”, Phys. Rev. Lett. **85**, 1548–1551 (2000).

[69] J.-J. Greffet, R. Carminati, K. Joulain, J.-P. Mulet, S. Mainguy, Y. Chen, ”Coherent emission of light by thermal sources”, Nature **416**, 61–64 (2002).

[70] G. S. Agarwal, ”Quantum electrodynamics in the presence of dielectrics and conductors. I. Electromagnetic-field response functions and black-body fluctuations in finite geometries”, Phys. Rev. A **11**, 230–242 (1975).

[71] V. M. Agranovich and D. L. Mills, *Surface Polaritons* (North-Holland, Amsterdam, 1982).

[72] S. Kawata (Ed.), *Near-Field Optics and Surface Plasmon Polaritons* (Springer, Berlin, 2001).

[73] E. W. Palik, *Handbook of Optical Constants of Solids* (Academic Press, San Diego, 1985).

[74] E. Wolf, "New theory of radiative energy transfer in free electromagnetic fields", Phys. Rev. D **13**, 869–886 (1975).

[75] W. H. Carter and E. Wolf, "Coherence properties of Lambertian and non-Lambertian sources", J. Opt. Soc. Am. **65**, 1067–1071 (1975).

[76] C. L. Mehta and E. Wolf, "Coherence properties of black-body radiation. III. Cross-spectral tensors", Phys. Rev. **161**, 1328–1334 (1967).

[77] F. Gori, D. Ambrosini, and V. Bagini, "Field correlations within a homogeneous and isotropic source", Opt. Comm. **107**, 331–334 (1994).

[78] H. M. Nussenzveig, J. T. Foley, K. Kim, and E. Wolf, "Field correlations within a fluctuating homogeneous medium", Phys. Rev. Lett. **58**, 218–221 (1987).

[79] S. A. Ponomarenko and E. Wolf, "Universal structure of field correlations within a fluctuating medium", Phys. Rev. E **65**, 016602 (2001).

[80] J. T. Foley, W. H. Carter, and E. Wolf, "Field correlations within a completely incoherent primary spherical source", J. Opt. Soc. Am. A **3**, 1090–1096 (1986).

[81] G. Gbur, D. James, and E. Wolf, "Energy conservation law for randomly fluctuating electromagnetic fields", Phys. Rev. E **59**, 4594–4599 (1999).

[82] G. K. Batchelor, *The Theory of Homogeneous Turbulence* (Cambridge University Press, Cambridge, 1970), Secs. 3.3 and 3.4.

[83] B. Karczewski, "Degree of coherence of the electromagnetic field", Phys. Lett. **5**, 191–192 (1963).

[84] B. Karczewski, "Coherence theory of the electromagnetic field", Nuovo Cimento **30**, 906–915 (1963).

[85] W. H. Carter and E. Wolf, "Far-zone behavior of electromagnetic fields generated by fluctuating current distributions", Phys. Rev. A **36**, 1258–1269 (1987).

Abstracts of Publications I-V

I. In near-field optics the resolution and sensitivity of measurements depend on the abundance of evanescent waves in relation to propagating waves. The electromagnetic field propagator is related to the scalar spherical wave, for which the Weyl expansion is a half-space representation containing both evanescent and homogeneous plane waves. Making use of these results we decompose the dyadic free-space Green function into its evanescent and homogeneous parts and show that some approaches put forward in the literature are inconsistent with this formulation. We express the results in a form that is suitable for numerical computation and illustrate the field decomposition for a point-dipole in some typical cases.

III. We investigate an extension to the concept of degree of polarization that applies to arbitrary electromagnetic fields, i.e., fields whose wavefronts are not necessarily planar. The approach makes use of generalized spectral Stokes parameters that appear as coefficients, when the full 3×3 spectral coherence matrix is expanded in terms of the Gell-Mann matrices. By defining the degree of polarization in terms of these parameters in a manner analogous to the conventional planar-field case, we are led to a formula that consists of scalar invariants of the spectral coherence matrix only. We show that attractive physical insight is gained by expressing the three-dimensional degree of polarization explicitly with the help of the correlations between the three orthogonal spectral components of the electric field. Furthermore, we discuss the fundamental differences in characterizing the polarization state of a field by employing either the two- or the three-dimensional coherence-matrix formalism. The extension of the concept of the degree of polarization to include electromagnetic fields having structures of arbitrary form is expected to be particularly useful, for example, in near-field optics.

III. We introduce the concept of degree of polarization for electromagnetic near fields. The approach is based on the generalized Stokes parameters that appear as expansion coefficients of the 3×3 coherence matrix in terms of the Gell-Mann matrices. The formalism is applied to optical near fields of thermally fluctuating half-space sources with particular interest in fields that are strongly polarized owing to resonant surface plasmons or phonons. This novel method is particularly useful when assessing the full vectorial characteristics of random evanescent fields, e.g., for near-field spectroscopy and polarization microscopy.

IV. We consider stationary electromagnetic fields modelled as superposition of unpolarized and angularly uncorrelated plane waves and show that in an isotropic case the electric cross-spectral tensor is proportional to the imaginary part of the Green tensor. This is as for black-body radiation but here the field need not be in thermal equilibrium. We also evaluate the degree of polarization for a homogeneous but non-isotropic field for which the plane waves propagate within a cone of angles. The results are compared with the known polarization properties of black-body radiation.

V. We investigate the structure of second-order correlations in electromagnetic fields produced by statistically stationary, homogeneous and isotropic current distributions. We show that the coherence properties of such fields within a low-loss or non-dissipative medium do not depend on the source characteristics, but are solely determined by the propagation properties, and that the degree of coherence of the field is given by the sinc law. Our analysis reproduces the known results for blackbody fields, but it applies to a wider class of sources, not necessarily in thermal equilibrium. We discuss the physics behind the universal behavior of the correlations by comparing the results with those obtained by an electromagnetic plane-wave model.

ISBN 951-22-6402-1